Cerebral Cortex August 2007;17:1766–1781
doi:10.1093/cercor/bhl088
Advance Access publication October 9, 2006

# First-In–First-Out Item Replacement in a Model of Short-Term Memory Based on Persistent Spiking

Randal A. Koene and Michael E. Hasselmo

Center for Memory and Brain, Department of Psychology and Program in Neuroscience, Boston University, Boston, MA 02215, USA

**Persistent neuronal firing has been modeled in relation to observed brain rhythms, especially to theta oscillations recorded in behaving animals. Models of short-term memory that are based on such persistent firing properties of specific neurons can meet the requirements of spike-timing–dependent potentiation of synaptic strengths during the encoding of a temporal sequence of spike patterns. We show that such a spiking buffer can be simulated with integrate-and-fire neurons that include a leak current even when different numbers of spikes represent successive items. We propose a mechanism that successfully replaces items in the buffer in first-in–first-out (FIFO) order when the distribution of spike density in a theta cycle is asymmetric, as found in experimental data. We predict effects on the function and capacity of the buffer model caused by changes in modeled theta cycle duration, the timing of input to the buffer, the strength of recurrent inhibition, and the strength and timing of after-hyperpolarization and after-depolarization (ADP). Shifts of input timing or changes in ADP parameters can enable the reverse-order buffering of items, with FIFO replacement in a full buffer. As noise increases, the simulated buffer provides robust output that may underlie episodic encoding.**

**Keywords:** gamma rhythm, integrate-and-fire neurons, persistent firing, sequence buffer, short-term memory, theta rhythm

## Introduction

Computer simulations of the encoding of a temporal sequence of spike patterns in recurrent neuronal networks often rely on a Hebbian model (Hebb 1949) of spike-timing–dependent potentiation (STDP) for the update of synaptic strengths. During learning, these simulations depend on the repeated presentations of spike patterns that are separated by time intervals smaller than about 40 ms, a window within which consecutive pre- and postsynaptic spikes were found to elicit long-term potentiation (Levy and Stewart 1983; Markram et al. 1997; Bi and Poo 1998). Yet in realistic experiments, a subject may be exposed to a sequence of stimuli that are separated by greater time intervals. One way to deal with this problem is to store each sequence in a short-term buffer that presents items at appropriate intervals. Because such a buffer cannot depend on synaptic modification for the temporary storage, we presuppose a mechanism of persistent spiking. The mechanism relies on after-depolarization (ADP), a membrane response that is intrinsic to many pyramidal cells of the entorhinal cortex (EC) (Klink and Alonso 1997a, 1997b; Egorov et al. 2002).

Computer models by Lisman and Idiart (1995) and Jensen et al. (1996) have simulated short-term memory (STM) function based on persistent spiking during modulation by theta rhythm. Chrobak and Buzsáki (1998) obtained elecrophysiological data during task performance that demonstrated nested oscillations at theta (8–9 Hz) and gamma (40–100 Hz) frequencies in EC, as well as similar activity in dentate, hilar, and hippocampal regions. These data also showed a phase-shifted synchronization of the oscillations in different regions. Previous simulations based on the Lisman and Idiart model did not deal with the dynamic characteristics of leaky spiking neurons and provided no mechanism for the ordered replacement of items in a buffer that is filled to capacity. Four-item capacity and replacement of items in a first-in–first-out (FIFO) manner are a good fit to the recency portion of graphs of serial position data (Atkinson and Shiffrin 1968; Kahana 1996). Psychophysical evidence for ordered item displacement has been gathered in tests ranging from precategorical acoustic storage (Crowder and Morton 1969) to observed interaction between memory load and item position for semantic information (Haarmann and Usher 2001). Earlier models incorporate functions that specifically attempt to fit this evidence (Phillips et al. 1967; Kahana 1996).

In prior work, we proposed buffer models that are related to the STM models by Lisman and Idiart (1995) that are based on persistent spiking, but we include more detailed simulation of the asymmetric distribution of spiking activity in each cycle of the 3- to 12-Hz theta brain rhythm (Koene 2006a, 2006b, in preparation), and we use leaky integrate-and-fire neurons to simulate neural dynamics (Koene et al. 2003). The implementation of the more realistic asymmetry has functional benefits: distinct portions of each theta cycle in a buffer can be synchronized with distinct modes of synaptic encoding and retrieval that alternate in each cycle of a theta rhythm in the recurrent networks that receive spike input from that buffer (Koene et al. 2003; Koene and Hasselmo 2005). By contrast, Jensen et al. (1996) relied on temporally separated periods of at least several seconds that are devoted exclusively to associative encoding or to retrieval in order to avoid interference between spiking in those 2 modes. Here, we add to the model a plausible mechanism for the FIFO ordered replacement of items that are maintained in the buffer as successive patterns of simultaneous spikes. Although Jensen et al. (1996) described a method by which items in the buffer could be replaced as new input appears, that proposal was not evaluated in simulations, and their proposed method relied on an even distribution of item reactivation spikes throughout a theta cycle. The mechanism proposed here performs the ordered replacement of buffered items, even when different numbers of simultaneous spikes represent each item, as may be expected for realistic stimuli. Our previously published studies involved the extensive use of an integrate-and-fire version of the STM buffer model in which pattern reactivation occurs specifically at the depolarized phase of theta modulation. Those studies focused on hippocampal (Hasselmo, Cannon, and Koene 2002; Koene et al. 2003) and

prefrontal cortex functions (Koene and Hasselmo 2005; McGaughy et al. 2005) during behavioral tasks in which the results of neuronal computation elicited dynamic responses from the task environment but did not deal specifically with the issue of patterns with different numbers of simultaneous spikes that represent the items maintained in STM.

Different numbers of neurons may spike to represent 1) the last item reactivated in the ordered buffer, 2) the insertion of a new item into the buffer by input, and 3) the first item that may need to be removed from the buffer. A mechanism of item replacement that is agnostic about numbers of spikes can use theta phase information to achieve the required functions. The necessary phase information is shown in Figure 1 for a theoretical 2-item buffer. Item replacement depends on the occurrence of spikes in both of 2 phases of the buffer cycle, namely, the last item phase indicated by (a) in Figure 1 and the input phase indicated by (b) in Figure 1. If this condition is met, then the item replacement mechanism must suppress spiking of any number of buffer neurons at the phase of the cycle indicated by (c) in Figure 1 at which spiking of a buffered first item would be reactivated.

In the following sections, we describe the STM buffer model, as implemented in the Catacomb (Cannon et al. 2003) simulation environment and its performance with different numbers of spikes representing individual items. The mechanism postulated for FIFO replacement of buffered items is then presented. The functional effects of significant changes of specific parameters of the STM model are analyzed, and modifications that lead to FIFO buffering in the reversed order of item presentation are demonstrated. Finally, the buffer model is shown to exhibit sufficient robustness in the presence of increasing levels of noise that affect spike timing to act as a useful STM when novel items need to be sustained for encoding in episodic memory.

## Methods

Our model is based on data suggesting that many pyramidal cells in layer II of entorhinal cortex (ECII) are specifically suited to reactivate firing patterns in a persistent manner due to intrinsic neuronal mechanisms. Such neurons exhibit an ADP of membrane potential after an action potential is elicited at the membrane. Klink and Alonso (1997a) showed that the ADP is caused by calcium-sensitive cation currents that are induced by muscarinic receptor activation. In addition to the ADP, activity in EC is modulated by a strong brain rhythm known as the theta rhythm that is present in behaving animals (Buzsáki et al. 1983; Fox et al. 1986; Fox 1989; Kamondi et al. 1998). In rats, for example, the theta rhythm has a frequency of about 6–10 Hz, which we represent in most simulations with 8 Hz. This rhythm may synchronize activity within a STM based on persistent spiking (Koene et al. 2003), and it may synchronize output to other regions such as region CA3 (Hasselmo, Bodelon, and Wyble 2002) or ECIII (Koene et al. 2003), where corresponding synaptic changes may occur. The reactivation of firing patterns by ADP in an ECII population of neurons between specific phases of each cycle of theta rhythm can therefore provide reliable input to other neuronal populations. Our model of STM in EC builds on a model first proposed by Lisman and Idiart (Lisman and Idiart 1995; Jensen and Lisman 1996a). In both models, recurrent inhibition separates the reactivation of sequential spike patterns in the buffer. The inhibition is provided by a population of interneurons, all of which spike in response to an action potential at any pyramidal cell in ECII (Bragin et al. 1995).

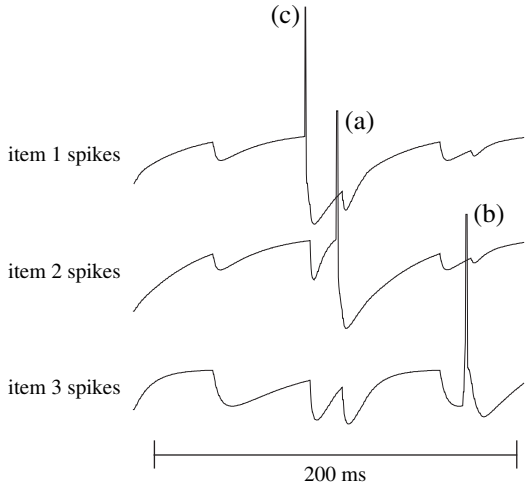


**Figure 1.** Detecting the need for item replacement due to activity at specific phases of theta modulation in a STM buffer based on persistent spiking. The buffer shown here is designed to hold a maximum of 2 items. Spikes at phases (c) and (a) represent items maintained in the buffer. The spike at (b) represents input that inserts a new item into the buffer.

### *A Leaky Integrate-and-fire Neuron Implementation of the STM Buffer*

Equation (1) shows how various contributions affect the response of model ECII pyramidal neurons and therefore their ability to sustain ordered sequences of spikes.

$$C\Delta v = \sum_i (g_i \Delta t (E_{\mathrm{rev},i} - (V + \Delta v)), \tag{1}$$

which can be rewritten as

$$\Delta v = \frac{\sum_i (g_i \Delta t (E_{\mathrm{rev},i} - V))}{C + \sum_i (g_i \Delta t)}, \tag{2}$$

where $C$ is the membrane capacitance, $\Delta v$ is the change of the membrane potential $V$ during a small time interval $\Delta t$, and $g_i$ is the conductance and $E_{\mathrm{rev},i}$ the reversal potential of a contributing membrane current. Capacitance and leak current determine the characteristic response of the membrane potential as it gradually returns to the resting potential. Below, we describe the contributing currents provided by rhythmic theta modulation, external afferent input to the buffer cells, intrinsic after-hyperpolarizing and after-depolarizing responses to action potentials, and inhibitory synaptic input from recurrent fibers of an interneuron network that is responsible for the observed gamma rhythm.

We use integrate-and-fire simulations of pyramidal cells of ECII, which have a membrane response with exponential decay to a resting potential $E_{\mathrm{rest}}$ = –60 mV due to membrane capacitance of $C$ = 1 mF and time constant of the leak conductance $\tau_{\mathrm{leak}}$ = 9 ms (the STM buffer has been shown to work with time leak constants between 8 and 19 ms. Below 8 ms, spike reactivation does not occur, whereas spikes may reactivate twice in one theta period when the time constant is above 19 ms, which leads to changes in the order of the spike patterns that are sustained in the buffer). The current contributed to the membrane potential by the leak conductance is defined by $E_{\mathrm{rest}}$ and the conductance $g_{\mathrm{leak}} = C/\tau_{\mathrm{leak}}$. The firing threshold is –50 mV, and the resting potential of –60 mV is chosen as the reset potential that follows a spike. Action potentials have a duration of 1 ms and are followed by a 2-ms refractory period and subsequent strong after-hyperpolarization (AHP). Many currents in equation (2), such as the AHP and synaptic input, are simulated with a fixed reversal potential $E_{\mathrm{rev},i}$ and a biexponential conductance response function

$$g_i(t) = G_i a_{\mathrm{norm}} (\exp(-t/\tau_{\mathrm{fall},i}) - \exp(-t/\tau_{\mathrm{rise},i})), \tag{3}$$

where $G_i$ is the characteristic amplitude of the conductance response for a specific membrane current, $\tau_{\mathrm{fall},i}$ and $\tau_{\mathrm{rise},i}$ are its fall and rise time constants, and $a_{\mathrm{norm}}$ is a normalizing factor to insure that the maximum value of $g_i(t)$ is $G_i$. The normalizing factor is computed by

$$a_{\mathrm{norm}} = 1/(\exp(-t\ \max/\tau_{\mathrm{fall},i}) - \exp(-t\ \max/\tau_{\mathrm{rise},i})), \tag{4}$$

where the time offset of the maximum response value is

$$t_{max} = \ln\left\{\frac{\tau_{fall,i}/\tau_{rise,i}}{(1/\tau_{rise,i}) - (1/\tau_{fall,i})}\right\}. \quad (5)$$

The AHP response approximates a single exponential function through a small rise time constant $\tau_{rise,AHP} = 10^{-4}$ ms and an exponential decay time constant $\tau_{fall,AHP} = 30$ ms with amplitude $G_{AHP} = 23$ ns and has a reversal potential of $E_{AHP} = -90$ mV. The biexponential ADP response has the shape of an alpha function with time constants $\tau_{rise,ADP} = \tau_{fall,ADP} = 125$ ms, amplitude $G_{ADP} = 30$ ns, and the reversal potential $E_{ADP} = -45$ mV. The ADP must rise over a time span that is approximately equal to the period of a theta cycle because reactivation of spikes on the rising flank of the ADP response insures that the order of spiking is maintained.

We model the rhythmic oscillation of the membrane potentials of pyramidal cells in ECII as inhibitory synaptic input that is modulated by rhythmic activity at a frequency of 8 Hz originating in the medial septum (Alonso et al. 1987; Stewart and Fox 1990; Skaggs et al. 1996; Wallenstein and Hasselmo 1997; Brazhnik and Fox 1999). The biexponential synaptic responses that cause this modulation have reversal potential $E_{theta} = -90$ mV, a conductance amplitude of $G_{theta} = 10$ ns, and time constants $\tau_{rise,theta} = 0.1$ ms and $\tau_{fall,theta} = 20$ ms. This gives the modulation of membrane potential the typical asymmetrical shape of the theta rhythm. The simulated 8-Hz theta rhythm is driven by septal spikes that commence at $t = 0$ ms.

An interneuron population in ECII is simulated by a single interneuron that receives fast connections (fast connections are simulated with a transmission delay of between 0 and 1 ms) from all pyramidal buffer cells and provides recurrent input to all pyramidal buffer cells. The interneuron responds rapidly to any buffer output spikes, due to biexponential synaptic input with the characteristic parameters $G = 30$ ns, $\tau_{rise} = 1$ ms, and $\tau_{fall} = 2$ ms, and a postsynaptic reversal potential $E_{rev} = 0$ mV. This "gamma" interneuron recuperates quickly due to a fast AHP response with $E_{AHP} = -90$ mV, $G_{AHP} = 100$ ns, $\tau_{rise,AHP} = 10^{-4}$ ms, and $\tau_{fall,AHP} = 4$ ms. The interneuron model also uses equations (1–5) but differs from that of the pyramidal cells due to reset and rest potentials $E_{reset} = E_{rest} = -70$ mV and a leak time constant $\tau_{leak} = 10$ ms. The competitive inhibition provided to pyramidal buffer cells by the model interneuron population simulates the postsynaptic response of γ-aminobutyric acid ($GABA_A$) receptors as a membrane current with $E_{gamma} = -70$ mV and a biexponential conductance response with characteristic parameters $G_{gamma} = 100$ ns, $\tau_{rise,gamma} = 0.1$ ms, and $\tau_{fall,gamma} = 2.5$ ms. The model of the network of interneurons in ECII was investigated in prior (Koene 2001) and related (Koene 2006b, in preparation) work.

The transmission of new input spikes to the buffer as well as the transmission of recurrent inhibition that is observed as a power variation in the gamma frequency band of the electroencephalography are modulated at theta frequency due to $GABA_B$ receptor activation by septal input at presynaptic terminals. In our simulations, the dynamic shape of the modulating amplitude, $f_{tmod}(t)$, is generated by the normalized output of a model neuronal membrane that receives synaptic input at theta frequency. The resulting transmission modulation has a scalloped shape typical of observed theta modulation. The transmission modulated conductance responses of input ($g_{input}(t)f_{tmod,input}(t)$) and of recurrent inhibition ($g_{gamma}(t)f_{tmod,gamma}(t)$) are 180 degrees out of phase. This means that input is suppressed during the reactivation phase of the buffer, at which time recurrent inhibition is needed to maintain the separation of successive spike patterns. Conversely, recurrent inhibition is suppressed when new input is received at the input phase of the buffer (which may initiate item replacement if the buffer is full). The period of greatest depolarization due to membrane currents produced by the theta rhythm (with $E_{theta}$ and $g_{theta}(t)$) is in phase with the strongest recurrent inhibitory transmission from the gamma interneuron population.

As in Lisman and Idiart (1995), spikes produced in ECII by stimulus input are reactivated repeatedly by the combination of ADP and positive theta modulation of membrane potential at a rate that matches the frequency of theta oscillation. A pattern of spikes that represents a stimulus input is maintained by this persistent spiking without any prerequisite synaptic connectivity. The persistent reactivation of a spike due to ADP is shown in Figure 2. The effect of ADP is modulated by acetylcholine (ACh), low levels of which do not support persistent firing (low ACh in Fig. 2). At high levels of ACh (high ACh in Fig. 2), stimulated buffer neurons can sustain firing at a rate that is determined by the time course of the ADP response. When ADP is combined with the alternating hyperpolarizing and depolarizing modulation of buffer neurons by the theta brain rhythm (high ACh + theta in Fig. 2), then persistent reactivation is phase locked within the cycle frequency of the theta rhythm. Rhythmic septal spikes that initiate each cycle of the membrane oscillation and the modulation of afferent and recurrent transmission have a 112-ms offset, whereas the first afferent can appear at $t = 125$ ms (i.e., input appears with a 13-ms relative phase offset after the peak of theta depolarization). The phase offset of all rhythmic input or modulation in the following paragraphs is given as an offset from $t = 0$ ms.

The membrane potentials of 3 neurons of a STM buffer are plotted in Figure 3. Theta oscillations define 2 functional phases of the buffer neurons. We call the phase interval of greatest rhythmic depolarization the reactivation phase of STM and the remaining interval the input phase of STM. The plots show that spiking produced by afferent activity during the input phase of the buffer is reactivated by the ADP during subsequent reactivation phases. The duration of the rise of ADP matches the period of oscillation. This means that the ADP of the earliest neuron to spike in one cycle allows that neuron to reach threshold first in the following cycle. The order of spikes is maintained during reactivation in STM. As spikes caused by output of the buffer occur in pre- and postsynaptic neurons of a target population with recurrent fibers such as entorhinal layer III or region CA3 of the hippocampus, an asymmetric function of STDP can take into account the order of spikes. This ensures that long term potentiation (LTP) (Bliss and Lømo 1973; Bliss and Collingridge 1993) is elicited in specific connections so that the order of events is maintained in episodic memory.

A rapid succession of septal spikes is used to suppress action potentials in the buffer neurons between trials of an experiment. This simulates the disappearance or resetting of theta rhythm as observed during context switches (Wyble et al. 2004). The buffer is cleared for the next trial.

### *A Phase-Locked Mechanism of FIFO Replacement of Buffered Items*

In the absence of input, the contents of a STM buffer decay gradually due to noise and a slow AHP (modeled as a biexponential response with $E_{rev} = -70$ mV, $G = 0.01$ ns, $\tau_{rise} = \tau_{fall} = 3000$ ms, an alpha function). When

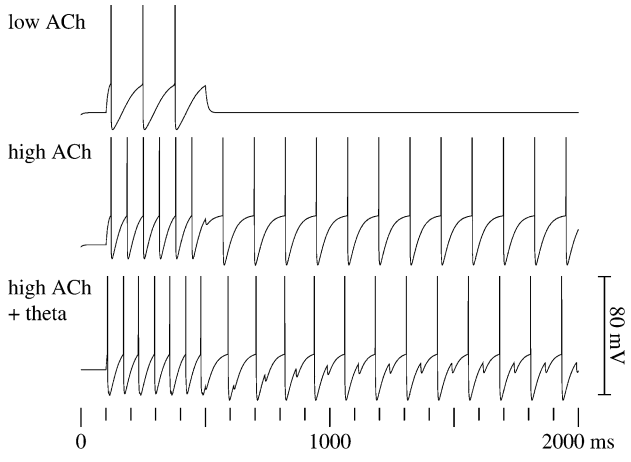


**Figure 2.** Simulated membrane potential of cells in ECII that exhibit cholinergic activation of sustained spiking activity due to an intrinsic ADP. Control condition, Low ACh: Spiking activity is elicited in neurons by a 400-ms current injection. The activity ends when current injection is terminated. High ACh: Spiking activity during current injection causes activation of a subsequent ADP due to the activation of muscarinic cholinergic receptors. Each spike is followed by a brief AHP, then an ADP that can lead to another spike. High ACh plus theta modulation: Spiking at regular intervals that is synchronized with theta rhythm results when the depolarizing phase of cholinergic theta modulation combines with ADP to elevate membrane potential to the spiking threshold. Intrinsic currents cause this sustained spiking, which does not depend on recurrent excitatory synaptic connections.

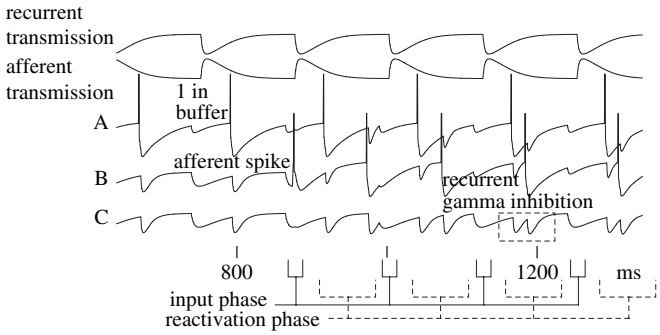


**Figure 3.** The buffer model operates in alternating functional phase intervals: 1) During a reactivation phase interval (bottom, dashed lines), modulation at theta frequency depolarizes pyramidal cells and ADP causes the reactivation of buffered spikes (A, B). The plots of recurrent and afferent transmission modulation (top) show that conductance through afferent input synapses is reduced during the reactivation phase, whereas the conductance of recurrent gamma inhibition is strong. This insures that reactivated spikes representing different items in the buffer are separated by competitive inhibition (highlighted in box on C response). 2) During an input phase interval (bottom, solid lines), modulation at theta frequency hyperpolarizes pyramidal cells, so that intrinsic spiking is inhibited. The plots of recurrent and afferent transmission modulation (top) show that conductance of recurrent gamma inhibition is reduced, whereas the conductance through afferent input synapses is strong. This enables afferent input to elicit new spikes in the buffer neurons (first spike on B).

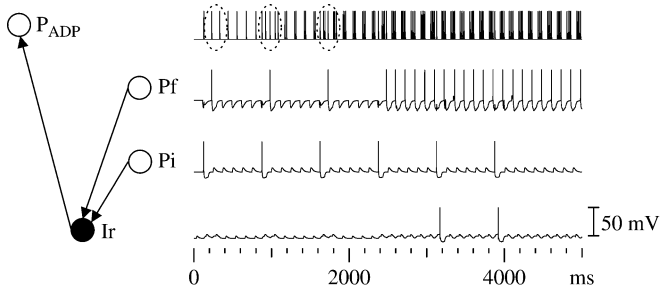


**Figure 4.** The membrane potential of the pyramidal neuron and interneuron populations involved in the proposed FIFO item replacement mechanism for the short-term buffer is shown. In this graph of our model of ECII, we use the unit $P_{ADP}$ to depict the main buffer pyramidal neurons that reactivate item spikes due to their intrinsic ADP currents. We depict a population of specialized pyramidal neurons as a single unit Pf that functions as a detector of a full buffer state. We depict another set of pyramidal neurons as a single unit Pi that functions as a detector of afferent input to the buffer. Septal input at theta frequency modulates the membrane potential of Pf and Pi neurons at the same phase as that of the $P_{ADP}$ buffer neurons. The efficacy of transmission through output connections from $P_{ADP}$ buffer neurons to Pf neurons is modulated at theta frequency, to strongly transmit only spikes of $P_{ADP}$ neurons at the theta phase interval of a reactivated fourth item in the buffer. During this phase interval, Pf spikes are elicited in the simulated full buffer detector when 1–8 inputs are received. The response trace of Pf neurons shows 3 spurious "full buffer" spikes (dotted circles). These spikes appear during the theta cycles that immediately follow first, second, and third item afferent input stimulation. In these cases, reactivated item spikes have yet to shift into earlier phases of the theta cycle. Pi spikes are elicited in the simulated afferent input detector when 1–20 simultaneous afferent inputs are received. The output of Pf and Pi neurons converges at specialized interneurons, here depicted by the Ir unit. The combination of input that signals a full buffer and afferent input elicits synchronized spikes of the Ir interneurons. The timing of these Ir spikes is controlled by the gating influence of septal input at theta frequency. This gating input has a phase offset that ensures that Ir spikes exert replacement inhibition at $P_{ADP}$ buffer pyramidal neurons at a specific theta phase, so that reactivation of the first item in the short-term buffer is suppressed. The response trace of Ir interneurons shows 2 occasions that elicit replacement inhibition spikes, namely, when the fifth and sixth afferent input stimuli appear.

a buffer that is filled to capacity receives new input at a rapid pace, so that the loss of spikes neither due to effects of noise nor due to slow AHP remove items from the buffer before the new input arrives, continued ordered buffering of the most recent spike patterns is only possible if a mechanism exists that can selectively remove the representation of the first item from the buffer to make room for a representation of the new item. If each item can be represented by a different number of simultaneous spiking pyramidal cells in the buffer, then the mechanism must be able to remove the first item regardless of how many and which neurons spiked to represent that item, and it must do this only when the buffer is full and new input arrives (if the buffer state is not detected and item replacement is elicited for every afferent input, then the effective buffer has the capacity to maintain one item). Neither the arrival of new input nor the "full" state of the buffer can be determined simply by detecting the activity of a certain number of spikes within a given time interval because the representations of the afferent input and of the reactivated items in the buffer may each consist of any number of spikes. In a buffer that depends on the timing of input and of gamma subcycles within each theta cycle, a reliable indicator of full buffer state and of an input event is the presence of spikes at specific phases of the theta cycle. In particular, spikes at the input phase of the theta cycle indicate the arrival of new afferent input and spikes at the reactivation phase of the *N*th item in a buffer with a capacity of *N* items indicate that the buffer is filled to capacity.

We therefore propose a FIFO ordered item replacement mechanism for the STM buffer that is robust with regard to differences in the number of spikes that represent specific items in the buffer. Our model for the replacement mechanism assumes that in addition to cells with ADP ($P_{ADP}$ in Fig. 4), ECII contains at least 3 other functionally distinct populations of neurons (schematically drawn as single nodes in Fig. 4, all with $E_{rest} = E_{reset} = -60$ mV). These are 2 populations of pyramidal cells (Pf and Pi in Fig. 4, both with $\tau_{leak} = 9$ ms and biexponential fast AHP responses with $E_{rev} = -90$ mV, $G = 10$ ns, $\tau_{rise} = 0.1$ ms, and $\tau_{fall} = 50$ ms) that do not exhibit ADP and one population of interneurons (Ir in Fig. 4, with $\tau_{leak} = 10$ ms) that is not already recruited to participate in the recurrent gamma inhibition.

Pyramidal cells of the Pf population receive as input (with biexponential postsynaptic responses at each synapse specified by $E_{rev} = 0$ mV, $G = 6$ ns, $\tau_{rise} = 0.1$ ms, and $\tau_{fall} = 1$ ms) the spikes produced by the pyramidal buffer cells (the $P_{ADP}$ trace in Fig. 4). This input is transmission modulated by activity on $GABA_B$ receptors on the terminals of the input synapses, so that the input gated in this manner is sensitive to the specific phase interval at which the reactivation of the *N*th item in the buffer normally occurs. The membrane potential of pyramidal cells in Pf is also modulated by theta rhythm (due to inhibitory biexponential responses with $E_{rev} = -90$ mV, $G = 10$ ns, $\tau_{rise} = 0.1$ ms, and $\tau_{fall} = 20$ ms) at the same phase as the modulation of the pyramidal cells that provide persistent spiking in the buffer. The synaptic strength of buffer input to the Pf population is tuned to cause spikes in Pf when one or more postsynaptic potentials are elicited, whereas the AHP of the Pf neurons prevents bursting when many simultaneous inputs are received. The Pf population functions as a full buffer state detector that is independent of the number of spikes that are reactivated during each theta cycle of the buffer, as demonstrated by the membrane response of Pf shown in Figure 4.

The capacity of the buffer is constrained by the phase offset of the transmission modulation that determines the *N*th item reactivation phase at which the Pf population detects a full buffer. In our implementation with an 8-Hz theta rhythm, the buffer is able to maintain up to 5 items (with some restrictions on the input protocol, as explained in the Discussion), and this maximum capacity is specified by a phase offset of 103 ms. A phase offset of 84 ms limits the capacity to 4 items, which is a robust capacity for this buffer. With a phase offset of 68 ms, the buffer capacity is limited to 3 items (in order to allow for some variability of spike timing, which includes the possibility of earlier spiking, the phase offsets were chosen to be 4 ms before the greatest offset at which a full buffer is consistently detected when the desired capacity is reached).

Pyramidal cells of the Pi population receive as input (with $E_{rev} = 0$ mV, $G = 6$ ns, $\tau_{rise} = 0.1$ ms, and $\tau_{fall} = 1$ ms) the spikes that provide afferent input to the buffer. Pi neurons also receive rhythmic excitatory input at theta frequency (with $E_{rev} = 0$ mV, $G = 2$ ns, $\tau_{rise} = 0.1$ ms, and $\tau_{fall} = 20$ ms) that is synchronized with the theta modulation of buffer pyramidal cells. This depolarization and the strength of synaptic input due to

afferent buffer input spikes are tuned so that Pi neurons spike when one or more afferent input spikes are detected. The AHP of Pi neurons prevents bursting when the input consists of multiple simultaneous spikes. The Pi population acts as an input detector that is independent of the number of spikes that represents the input, as shown in the Pi membrane response trace in Figure 4.

The interneuron population Ir also receives excitatory input (with a biexponential postsynaptic response with $E_{rev}$ = 0 mV, $G$ = 1.2 ns, $\tau_{rise}$ = 0.1 ms, and $\tau_{fall}$ = 10 ms) at theta frequency, at a phase offset (32 ms) that depolarizes the interneurons in synchrony with the expected reactivation phase of the first item that is maintained in the buffer. Input of spikes generated by the Pf pyramidal population is received at synapses with slow biexponential timing constants of the postsynaptic response ($E_{rev}$ = 0 mV, $G$ = 0.5 ns, $\tau_{rise}$ = 20 ms, and $\tau_{fall}$ = 60 ms). Therefore, depolarization by that postsynaptic potential can combine with input of spikes from the Pi pyramidal cells at synapses with faster biexponential response timing ($E_{rev}$ = 0 mV, $G$ = 0.5 ns, $\tau_{rise}$ = 10 ms, and $\tau_{fall}$ = 60 ms) to elicit spiking in the population of interneurons (Ir membrane response trace in Fig. 4). When input indicates both a buffer filled to capacity and the arrival of afferent input, spiking of the Ir interneurons (limited by an AHP with $E_{rev}$ = –90 mV, $G$ = 4 ns, $\tau_{rise}$ = 4 ms, and $\tau_{fall}$ = 50 ms) provides GABAergic inhibitory input to all intrinsically spiking buffer neurons ($P_{ADP}$ in Fig. 4) through synapses with reversal potential $E_{rev,Ir}$ = –90 mV, conductance amplitude $G_{Ir}$ = 40 ns, and biexponential time constants $\tau_{rise,Ir}$ = 1 ms and $\tau_{fall,Ir}$ = 5 ms. This replacement inhibition specifically suppresses spikes at the phase interval during which the ADP of the spikes that represent the first item maintained in the buffer could elicit reactivation spikes. As the ADP begins to decline, spiking is no longer possible and the item is removed from the buffer. The buffer can then support the maintenance of the new item, as ADP reactivates the spikes elicited by afferent input as the last pattern of spikes in the buffered sequence.

In order to achieve complete first item suppression through a short replacement inhibition at the first item reactivation phase, specific conditions must be met: 1) At first item reactivation time, $t_{fr}$, the contributions of theta plus ADP begin to elevate membrane potential above the firing threshold. 2) At times $t \geq t_{fr}$, the combined contributions of theta modulation plus ADP plus gamma inhibition always lead to membrane potential below the firing threshold. These 2 conditions are met if the time interval between the previous reactivation time of the first item and $t_{fr}$ is approximately equal to the time taken to reach peak ADP and if theta modulation is flat or its contribution increases more slowly than the contribution of ADP decreases after $t_{fr}$ (if the ADP response exhibits a steeper decline, then a greater proportion of each theta cycle may be used for item reactivation. A more rapid termination of the effect of an intrinsic response [such as the ADP] may be achieved by providing an opposing current with an onset at the desired time of termination [such as an inhibitory postsynaptic potential]).

## Results

A buffer mechanism for sequences of spike patterns that is independent of synaptic connectivity is necessary for their encoding in episodic memory. In a realistic setting, the spike patterns that make up a sequence to be encoded in episodic memory may be elicited by input stimuli with intervening time intervals of arbitrary duration. The Hebbian process of STDP depends on pre- and postsynaptic spiking that occurs within a time interval of at most 20–40 ms (Levy and Stewart 1983; Markram et al. 1997; Bi and Poo 1998). Therefore, a buffer that repeatedly reactivates a time-compressed version of a sequence of spike patterns is ideally suited to meet the requirements for encoding in episodic memory.

Initial simulations illustrated problems with the absence of an item replacement mechanism. Figure 5 shows how distinct input and reactivation modes appear in the persistent spiking buffer and that FIFO replacement is not accomplished simply by adding new input to a full buffer, as was suggested for item replacement in Jensen et al. (1996).

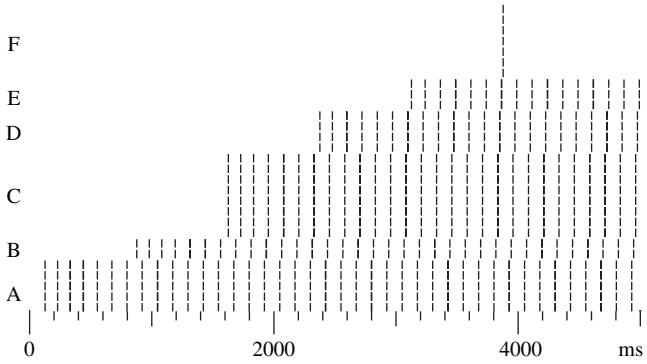


**Figure 5.** A simulation that shows the performance of a buffer with a maximum capacity of 5 items and no item replacement mechanism as a sequence of 6 spike patterns (A–F) is elicited by afferent input that appears at intervals of 750 ms. The items are represented by patterns consisting of different numbers of simultaneous spikes. New items appear more rapidly than buffered items would terminate due to the slow AHP that is included in the model. Items A–E are maintained in the order of their appearance, but the depolarizing phase of theta modulation ends before the spiking representation of item F can be reactivated in the buffer. Without replacing the oldest item in the buffer, the sixth item does not interfere, but is not maintained in the simulation of STM either.

### *Testing Buffer Function and the Replacement Mechanism*

A simulation of buffer performance with the proposed FIFO item replacement mechanism is shown in Figure 6. The spiking representations of successively presented items (A–F) were acquired in the buffer, and STM was maintained by persistent firing, without synaptic modification. Input spikes (see the afferent spike for item E in Fig. 6*c*) were presented only once, and item representations consisted of different numbers of simultaneous spikes. Figure 6*a* shows that representations with 2–8 spikes were maintained in order by a buffer that used a single interneuron model to achieve competitive inhibition. The inhibition appears as a visible gamma oscillation superimposed on the theta rhythm in Figure 6*c*, during the reactivation of item representations. The sequence of reactivation maintained the order but compressed the time between successive item presentations.

Figure 6*c* indicates that the timing of spiking in the model would allow STDP to modify synapses between neurons that are activated by the output of the buffer in order to achieve autoassociative encoding of item representations. The buffer output may also enable episodic encoding with greater STDP time windows (Koene et al. 2003; Koene and Hasselmo 2005), in which synaptic strengthening by STDP depends on the size of the time interval between spikes (Jensen and Lisman 1996b; Koene 2006a, in preparation). Figure 6*b*,*c* shows the spiking of replacement interneurons (I) and the consequent suppression of the first set of persistent spikes. Replacement inhibition removed the representation of item A as item E appeared and removed the representation of item B as item F appeared, so that a buffer capacity of 4 spiking item representations was achieved. In each case, the spike representation of the new item reactivated to take the last position in the buffered sequence.

### *The Significance of Characteristic Model Parameters*

We may predict functional changes that result from modifications of specific characteristic parameter values of the buffer model. Transmission modulation of the input to pyramidal cells

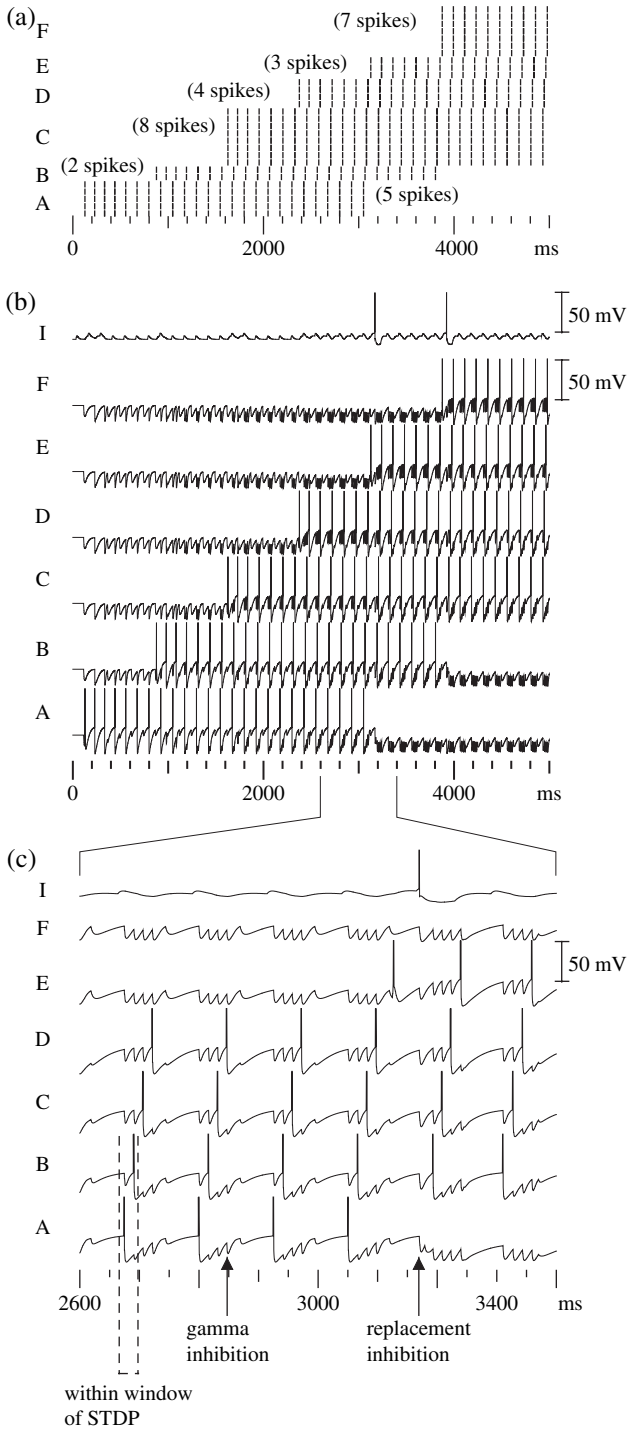


**Figure 6.** A simulation that shows buffer performance and FIFO item replacement with a STM model that has a 4-item capacity as a sequence of 6 spike patterns (A–F) is elicited by afferent input that appears at intervals of 750 ms. (*a*) Each item is represented by a different number of simultaneous spikes (from A to F: 5, 2, 8, 4, 3, and 7 spikes), each of which is shown as a short vertical line in the spike plot. Each pattern of spikes is acquired by the buffer, and the spikes are reactivated simultaneously, with visible phase offsets between consecutive patterns in a buffered sequence. When the fifth pattern of spikes (E) appears, the pattern representing A does not reactivate. When the sixth pattern (F) appears, B is no longer maintained. (*b*) Plots of the membrane potential of the first spiking neuron in each item representation (A–F) show regular modulation in each theta cycle. The membrane potential plotted in I shows spikes of the interneuron population that provides replacement inhibition when new spikes appear in a full buffer due to afferent input. (*c*) At a greater temporal resolution, plots of membrane potential show the functional significance of the timing of the spikes in the buffer. Reactivated spikes of consecutive items maintained in the buffer fall within a time interval small enough so that output from the buffer to a neuronal network with recurrent connections can enable synaptic modification by spike-timing–dependent plasticity that encodes episodic relationships between patterns of spikes. Recurrent gamma inhibition maintains the separation and therefore the order of reactivated patterns of spikes. The time interval of the separation is on the order of the cycle period of observed gamma rhythm. When interneurons I spike, replacement inhibition hyperpolarizes all intrinsically spiking pyramidal cells in the buffer. Without this hyperpolarization, the reactivation of spikes that represent the first item in the buffer occurs at the peak of the neuronal ADP response. When hyperpolarized during replacement inhibition, the ADP begins to decay. The spikes representing A no longer reactivate. The buffer then maintains representations of items B, C, D, and E.

in the full buffer detector (Pf in Fig. 4) is a critical variable of the proposed mechanism. We predict that such transmission modulation exists in ECII. If it does not, then the alternative approach is to supply phase-specific filtering through strong theta modulation of the pyramidal cells in the full detector. This modulation can take the form of rhythmic excitatory and/or inhibitory input.

Transmission modulation of the recurrent inhibition that is observed as gamma rhythm is not critical, as it merely limits how close together afferent input and the first item reactivation can appear. Without mode-specific modulation, the recurrent gamma inhibition that occurs as a result of pyramidal spikes elicited by afferent input imply that a minimum interval must lie between the afferent input spikes and the first item reactivation spikes (Fig. 7). In the special case of a type of reverse-order STM buffer that depends on the phase of afferent input (demonstrated in Fig. 8), proposed transmission modulation of recurrent inhibition may affect buffer function.

The buffer works with AHP conductance values between 25 and 35 ns. If the AHP is too strong, it suppresses reactivation (especially reactivation in the same theta cycle, as is necessary when new input is received in the STM buffer). If the AHP is too

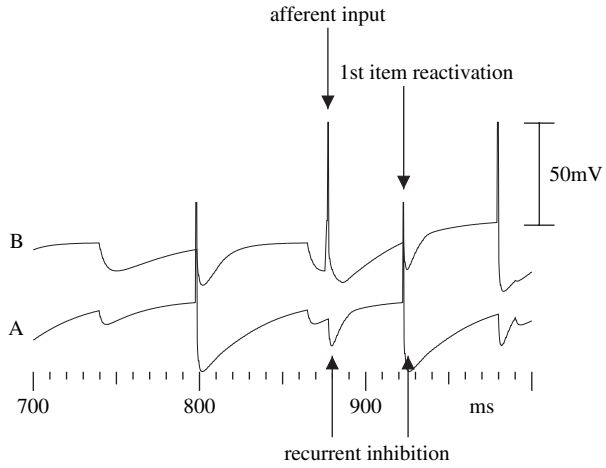


**Figure 7.** Simulated membrane potential of 2 pyramidal cells in ECII, in the absence of proposed theta modulation of recurrent gamma inhibition. Neuron A spikes rhythmically as a member of the first pattern of spikes maintained in STM. When a second pattern of spikes is introduced to the buffer, afferent input causes a spike in neuron B. Without transmission modulation, this spiking elicits interneuron activity that produces inhibition of the pyramidal cells through recurrent fibers. If spikes due to afferent input occur in an early phase of the theta cycle and if the duration of recurrent inhibition is sufficiently brief, then the reactivation of spikes in the first buffered item is not suppressed.

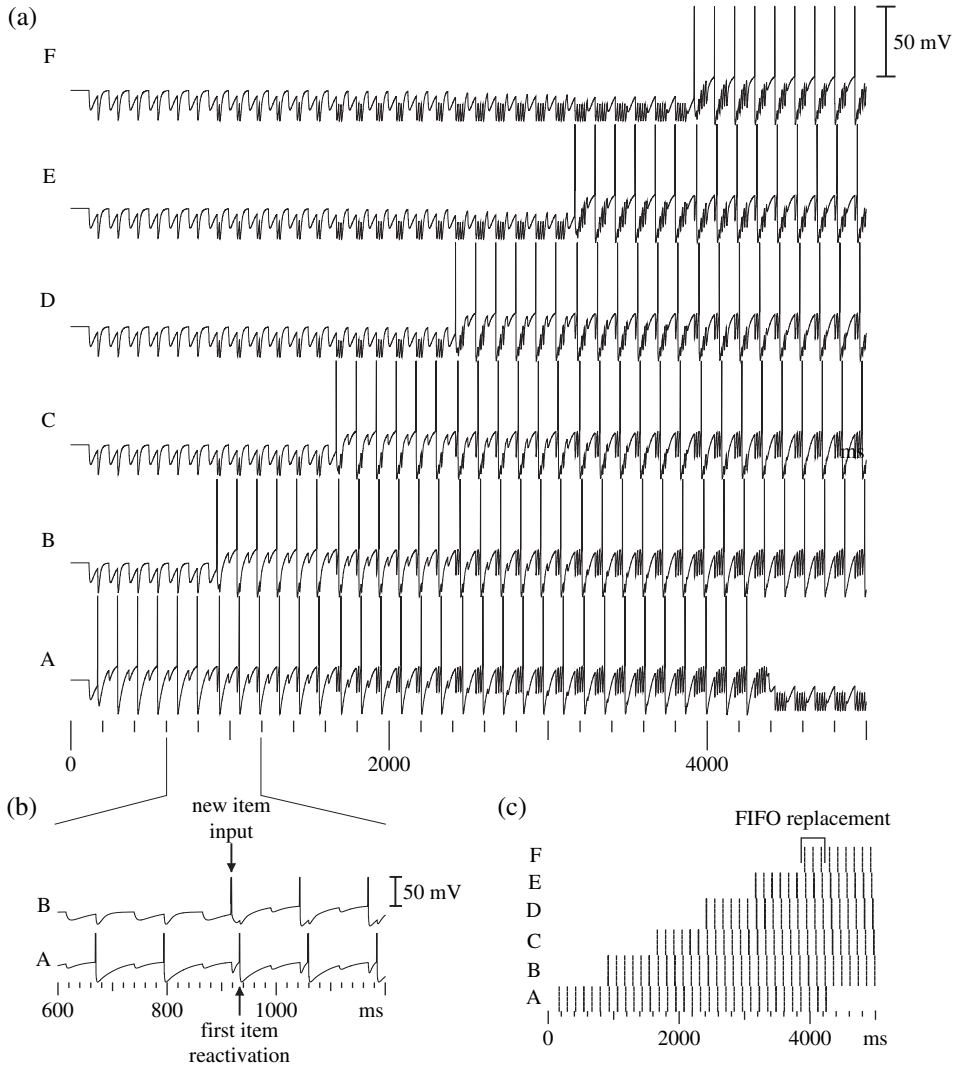


**Figure 8.** A simulated reverse-order buffer, in which the reversal of the order of item presentation is a consequence of the late phase of afferent input to the buffer. (*a*) Plots of the membrane potential of one of the spiking neurons in the buffered representations of each item (A–F) show that new spikes appear at a short time interval before the reactivation of spikes maintained in the buffer. The spikes representing buffered items reactivate in the reverse order of their presentation to the buffer. Item A drops out of the buffer a few theta cycles after item F appears. This shows that FIFO item replacement is achieved without an explicit replacement mechanism, as the spikes representing A are shifted beyond the depolarizing phase of the rhythmic membrane modulation at theta frequency. (*b*) When the phase of afferent input precedes the reactivation phase of the first item in the buffer with only a short time interval, the ADP of the neurons that spike as novel input is received is unable to elicit reactivation within the same theta cycle. If the rise time of the ADP is slightly greater than the duration of a theta cycle, then the neurons that spike for B will have a greater depolarization than those that spike for A at the onset of the next period of rhythmic depolarization. In that theta cycle, B therefore reactivates before A. (*c*) This reversed order of reactivation is then maintained in the buffer for all patterns of simultaneous spikes that represent items A–F.

weak, then different combinations of ADP and theta modulation are needed for a functioning buffer, otherwise a spike pattern may appear more than once in a theta cycle, which causes a deterioration of the order and distinctness of items maintained in the buffer. Changing the conductance or the fall time of the AHP can both change the effective strength of the AHP, with consequences as described above.

An ADP rise time of 90–160 ms results in a working buffer. Our evaluation of the buffer model indicates that there is some room for variations of the intrinsic characteristics. The buffer model does not require extreme fine-tuning of physiological parameters, so that neurons with a range of acceptable characteristic parameter values can participate as buffer neurons in ECII. Buffer function requires precision for phase locking in the following parameters: 1) The phase at which input is received by the buffer. 2) The phase at which a full buffer is detected. 3) The phase at which replacement inhibition occurs in the buffer. Fortunately, phase-specific sensitivity can be learned.

### *Reverse Buffering*

The buffer reactivated and maintained a sequence of spikes in the reverse order of their initial presentation when a specific relationship of characteristic parameters was used, as shown in Figures 8 and 9. This function is predicted if the rise-time constant and amplitude of the ADP response are such that a new input spike does not lead to a reactivation spike within the same theta cycle. If neurons exist that respond in this way, then a reverse-order persistent spiking buffer provides a mechanism for the repeated presentation of item spikes needed to establish

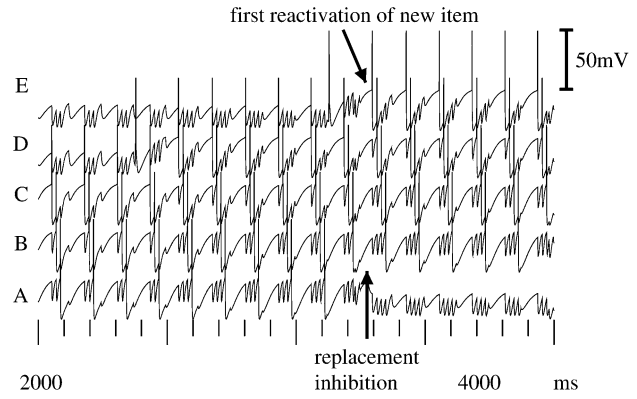


**Figure 9.** A simulated reverse-order buffer, in which the reversal of the order of item presentation is a consequence of the time constants used for the model ADP response. Membrane potential is plotted for one neuron involved in the spiking representation of each item A–E. A slow rise of the ADP means that spikes representing E, caused by afferent input, do not reactivate within the same theta cycle. A rising ADP is maintained until spiking is possible during the next theta cycle, at which time the replacement mechanism suppresses reactivation of spikes representing item A. As the ADP is still rising, the neurons of E spike before the remaining reactivated spikes. A reverse order of reactivation is then maintained in the buffer for the patterns of spikes that represent items B–E.

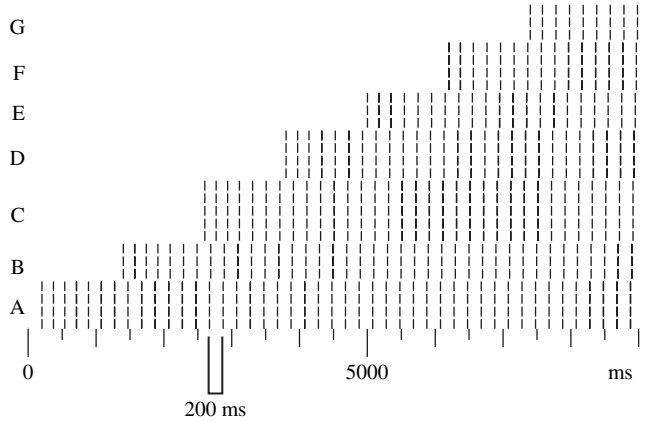


**Figure 10.** Simulated patterns of spikes for 7 items (A–G) maintained in a STM buffer with a longer theta frequency (5 Hz). The time span of each theta cycle is 200 ms, and each cycle includes a phase of pyramidal depolarization of greater duration than the depolarized phase in a buffer with 8-Hz theta rhythm. The strength of gamma inhibition was not modified, so that the maximum number of spike pattern that can be reactivated in the depolarized phase of theta rhythm and reliably separated by gamma intervals is increased. This gives the buffer the robust capacity to maintain 7 items, plotted as different numbers of simultaneous spikes for items A–G.

a backward association with spike-timing–dependent plasticity. When learning from realistic training input in which the stimuli of one trial are presented once in a specific order, such backward associations are needed in models of goal-directed behavior that rely on converging forward and reverse spread of activity through neurons, each of which represent an item in a sequence of encountered items (such as places or stimuli) (Hasselmo 2005; Koene and Hasselmo 2005), or in models of context-dependent retrieval of episodes (Hasselmo and Eichenbaum 2005).

### *The Effect of the Theta Frequency and of the Strength of Competitive Inhibition on Buffer Capacity*

In Figure 10, we show that the capacity of the buffer is increased to 7 items when we lower the frequency of the theta rhythm that septal inputs are assumed to provide to 5 Hz. By retaining the same strength of the recurrent inhibition in the network, more gamma cycles were nested within the depolarizing reactivation phase interval of the extended theta cycle duration.

When instead we manipulate only the conductance parameter for the inhibitory response produced at pyramidal cells due to recurrent input from the gamma interneuron network, we show that strengthening that inhibition leads to a smaller capacity of STM (Fig. 11). Stronger gamma inhibition delays the spiking of successive spike patterns maintained in the buffer, which results in a lower observed gamma frequency. Fewer gamma cycles at that frequency fit into the depolarizing reactivation phase interval of the theta rhythm.

Conversely, the capacity of STM may be increased if gamma inhibition is weakened. Given a specific theta frequency, the capacity of STM that can be achieved in this way is limited by a critical value for the strength of recurrent gamma inhibition. Below this value, the competitive inhibition that one pattern of pyramidal spikes elicits by activating the gamma interneuron network is insufficient to maintain separation from the following pattern of buffered spikes by a minimum time interval. In

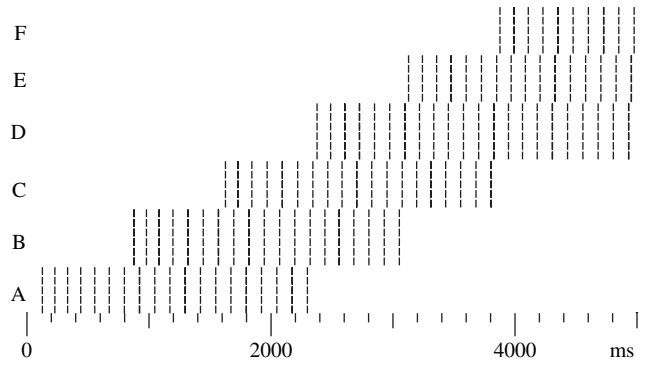


**Figure 11.** Simulated patterns of spikes in a STM buffer with capacity limited by greater strength of gamma inhibition ($G_{gamma}$ = 480 ns). Six patterns of simultaneous spikes representing items A–F are presented as input to the buffer. A sequence of 3 of these patterns of spikes can be sustained in the order of presentation by persistent firing.

Figure 12, we show that STM function deteriorates with weak gamma inhibition ($G_{gamma}$ < 2.5 ns). After few theta cycles, initially distinct patterns of spikes merge to spike simultaneously. For reliable buffer performance, a greater minimum strength of gamma inhibition is needed when we take into account the influence of noise in biological systems, such as in several of the simulations described in following results.

### *The Effect of Interference between Item Representations*

We considered the case where the sets of spikes that are consecutively elicited by a sequence of afferent input are not completely distinct. A pyramidal cell of the buffer that has spiked and experiences ADP may spike due to afferent input. When that happens, the ADP response is reset in order to model the resetting of internal calcium concentration of the cell as a consequence of the spiking action. The afferent input therefore determines the new phase of the buffer cycle at which a spike is reactivated, and this spike no longer contributes to the same

representation of a buffered item. This is shown for the case of 2 items with overlapping spiking representations, C and F in Figure 13. When the spiking representation of F entered the buffer, the representation of C was reduced to a smaller subset of spikes (C′). If C is a known item that has been previously encoded in a recurrent network, then the reduction of C may be countered by autoassociative retrieval into the buffer (Koene 2006b, in preparation). The spike representation and reactivation of the new item F were not affected.

If afferent input causes spikes that match the complete representation of a buffered item, then that item will reactivate only in the temporal order (buffer position) of the new input. The original temporal position of the item representation that reappeared while buffered is lost and the sequence shifts to fill the blank location. If the same input is presented multiple times consecutively, then buffer content will not appear to change and will contain only one instance of the corresponding item representation. No effect is noticeable if novel input presents the same set of spikes that represent the first item in a buffer that is filled to capacity.

This loss of a previous instance of an item representation that matches new input was simulated in prior work for a delayed nonmatch to sample task (McGaughy et al. 2005) to show that it may explain specific errors in the observed behavior of rats

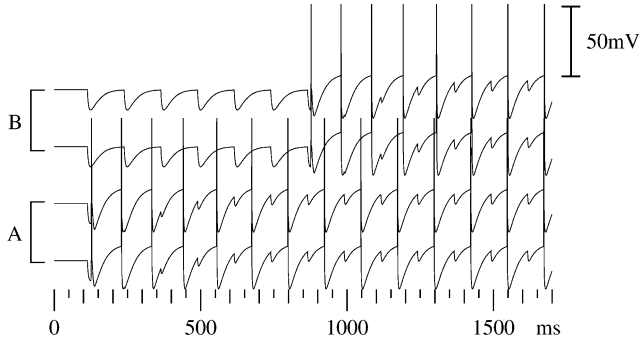


**Figure 12.** The membrane potential of 4 pyramidal buffer neurons, of which pairs spike as members of 2 separate patterns that represent items A and B. The separation is maintained for 5 theta cycles, after which all 4 spikes are reactivated nearly simultaneously, in effect merging the buffered representations of A and B. The loss of separation occurs due to insufficient strength of recurrent gamma inhibition.

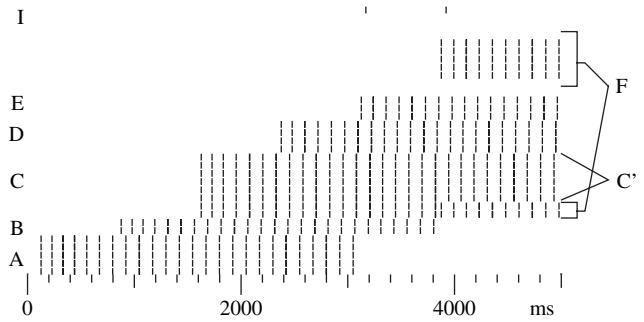


**Figure 13.** Spikes of a short-term buffer simulation with 6 item representations (A–F), of which 2 (C and F) share a subset of spikes. Spikes labeled I show when the interneurons of the replacement mechanism spike to cause suppression of the first item in the buffer. The spike representation of item F includes 5 novel spikes and 2 spikes that previously contributed to the representation of item C. As item F appears, the reactivation of spikes representing B is extinguished and the set of spikes that are reactivated in ensuing theta cycles to represent C is reduced to 6 spikes (labeled C′). Novel and overlap portions of the spike representation of F reactivate in the proper order, as the most recent and therefore the last item maintained in the buffer.

(McGaughy et al. 2004). In the experiment, rats were trained to sniff consecutively at 2 different odors (A and B). Following a delay, the rats were given a test odor, after which the task required that the rat dig in one of the original 2 containers to point out the one with the nonmatching odor. Rats with prefrontal cortex lesions, but intact EC, displayed a peculiar performance error. If trained rats were presented with odors A and B, then with a test odor matching A, they had no difficulty identifying the separate test container with odor B. When these rats were given a test odor matching the second of the 2 sample odors (B), then they were confused by the repetition and were unable to perform the task. They eventually picked a container at random (chance-level performance).

We propose that the observed inability of lesioned rats to perform the nonmatch to sample task may be explained by reliance on a buffer with 2 specific characteristics: 1) Only one instance of a specific pattern of spiking neurons can be maintained as part of a buffered sequence. 2) Presenting a novel pattern of spikes may cause the displacement and therefore the forgetting of a previously buffered item representation. The effect of these 2 functional constraints is demonstrated most clearly in a simplified simulation where the sequence buffer of a virtual rat has a capacity of only 2 items.

For virtual rats with the simplified 2-item buffer, our model predicts that a reduction of buffer content is caused by the presentation of the same stimuli that elicited maintenance of that last (i.e., second) item in the buffer. As explained above, this is predicted for all cases where spiking due to new input matches a spiking representation that is maintained in the buffer. Each buffered item may represent knowledge of an odor and an associated container. When the test phase involves input of B, then the replacement mechanism removes A from the full buffer. Only one item (B) remains in the buffer. According to our model, the rats with prefrontal lesions are left with insufficient information in that case to perform the 2 comparisons that are expected in the delayed non-match to sample task.

We do not wish to imply that the full capacity of the short-term buffer in rats is 2 items, so we follow the 2-item example with a simulation where the capacity is a more plausible 3 items. In that case, we presume that the third buffered item represents some interceding event, such as a perception of the switch from sample presentation to the delay and performance parts of the task. We show the results of simulation with both capacities, 2-item capacity in Figure 14*a* and 3-item capacity in Figure 14*b*. Simulating a buffer limited to 2 items is done with a phase offset of 53 ms for the transmission modulation of buffer output into neurons detecting the full buffer state, and the conductace amplitude of the input from these detector neurons to the replacement interneurons is raised to $G = 1.0$ ns.

### *A Reliable Model of STM Deals Gracefully with Noise*

We evaluated the effect of noise on the function of the STM buffer when the reactivation of novel patterns of simultaneous spikes relies entirely on persistent firing without synapse-dependent retrieval. Noise was added through simulated current clamps of individual neurons driven by a first-order autoregressive process (a model for the response to noise that is similar to a random walk) with Poisson distribution, a mean value of 0, amplitude 1 pA, and regression parameter 0.5. With this noise, we evaluated the statistical probability of errors in

the buffered patterns of spikes by performing 50 simulation runs, each over 5000 ms, presented with 6 stimuli that were represented by patterns consisting of between 2 and 8 simultaneous spikes with a total of 28 active neurons. Of the 50 runs, 27 simulation runs produced no errors. The mean error quantified as all missing or extra spikes at the end of a simulation run was 1.22 spikes with a standard deviation of 1.8 (a bit error rate of 0.044). The first item pattern presented to the buffer contained errors in 15 of the 23 runs that exhibited errors due to noise. In only 2 of the simulation runs did more than one spike pattern contain errors. In both of these runs, the number of patterns involved was 2, and in both cases, the first item pattern presented to the buffer was one of these. Never was an entire spike pattern lost to noise.

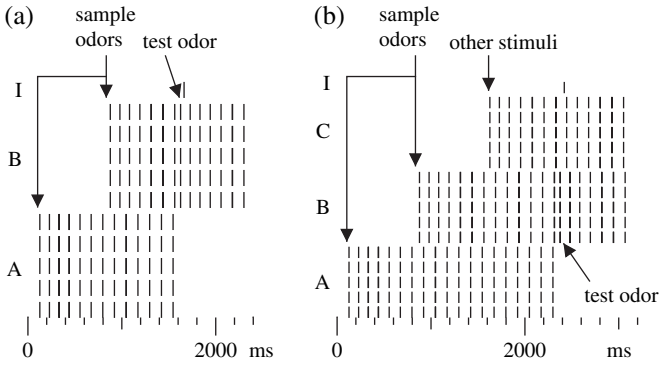


**Figure 14.** Spikes of the replacement interneuron and item representations A, B, and C. (*a*) In a buffer with 2-item capacity, sample odors A and B cause afferent input that elicits representative spikes, which are maintained in a buffer model of ECII. A test odor that matches B is then presented. The afferent input causes replacement interneuron spiking in the full buffer, so that the representation of odor A is removed from the buffer. Only a spike representation of odor B is maintained. (*b*) In a buffer with 3-item capacity, a third spike representation is elicited by other stimuli, preceding the delayed presentation of the test odor. Once the test odor is presented, the representation of odor A is removed and only the representation of odor B is maintained.

During some simulation runs, individual spikes of the first pattern in the STM buffer stopped reactivating if noise delayed reactivation sufficiently so that the competitive recurrent inhibition caused by the remaining spikes suppressed reactivation of the delayed spike until its ADP began to fall. In effect, the spike was removed from the buffer in the same manner as items are removed by the replacement mechanism (Fig. 15). A similar error appears occasionally in items other than the first if reactivation in the same theta cycle as the presentation of afferent input fails.

When noise produces a delay in the reactivation of individual spikes, delayed spikes may end up in a separate gamma cycle, effectively adding another item in the buffer that is then sustained in that order (Fig. 16). For novel items, encoding with such noise effects may separate a single item representation (normally stored through STDP by the strengthening of autoassociative synaptic connections) into multiple parts that are subsequently stored as an episode.

In general, the first item in the STM buffer is more susceptible to noise-induced errors than the following items that are flanked by gamma inhibition and for which reactivation is driven by combinations of depolarization by theta modulation and ADP that significantly exceed the threshold potential. The membrane potentials of these items exceed the threshold potential before reactivation of spiking, as their spiking is actively delayed by recurrent inhibition. It is notable that even in the presence of relatively strong noise (with values up to ±10 pA), several of the spikes in each item pattern tend to survive the difficult insertion into the buffer and continue to reactivate in the correct order (Fig. 17*a*). As even stronger noise is added (values that reach ±60 to ±70 pA), the duration of item maintenance in the STM buffer is limited by the dropout of spikes (Fig. 17*b*).

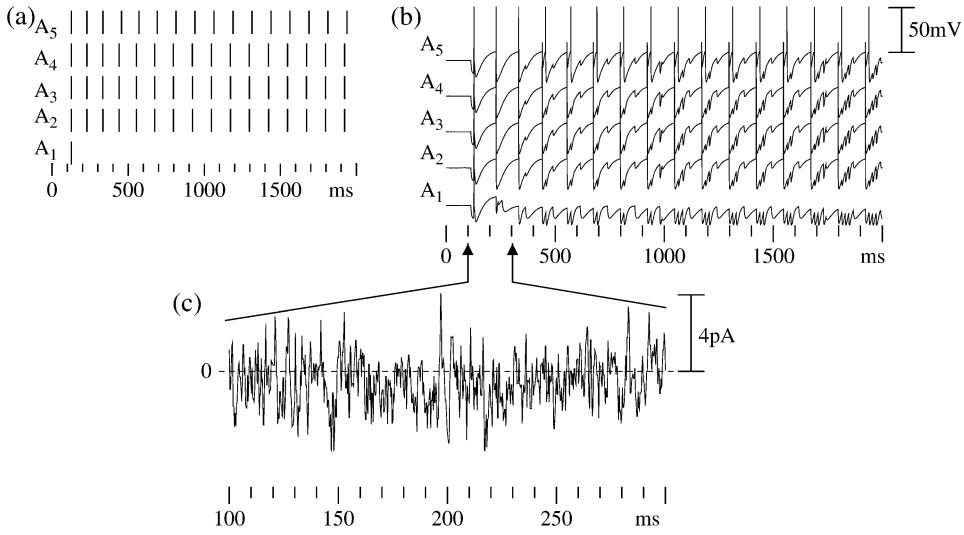


**Figure 15.** The dropout of individual spikes during the presentation of novel input to the buffer in the presence of noise that affects neuronal membrane potentials. (*a*) The spikes of 5 pyramidal buffer cells that fire in response to afferent input at $t = 125$ ms are plotted. Spiking in neurons $A_2$–$A_5$ is reactivated rhythmically with minor timing variations due to noise. However, because of the noise, the initial spike in neuron $A_1$ is not reactivated so that this neuron drops out of the pattern of spiking neurons that represents item A. (*b*) A plot of membrane potentials of the pyramidal cells shows that a momentary reduction of the membrane potential of neuron $A_1$ during the depolarizing phase of theta modulation delayed its elevation by peak ADP to the threshold potential. The spikes of $A_2$–$A_5$ caused competitive inhibition through the recurrent fibers of the gamma interneuron network, further suppressing the membrane potential of $A_1$. Following this suppression, the decaying ADP of $A_1$ could not reach the spiking threshold. (*c*) A plot of the simulated autoregressive noise, which decreased the membrane potential of $A_1$ at a critical phase of the theta cycle and thereby effectively removed that neuron from the buffered representation of item A.

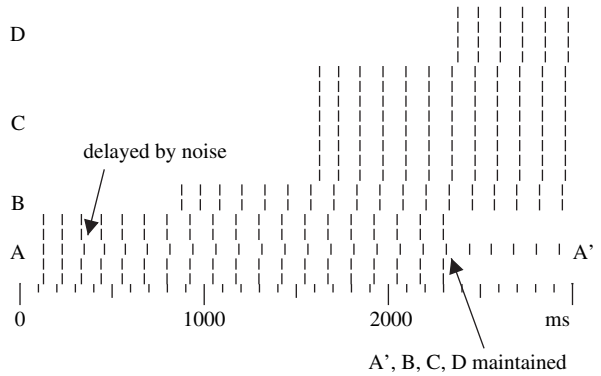


**Figure 16.** Plots of the spike patterns that represent buffered items A–D show that spiking that is delayed by noise, but does not cause spike dropout, can establish separately sustained spiking. The spikes denoted by A′ effectively split the original spike pattern representing item A into 2 consecutive spike patterns. The split may also affect the perceived capacity of the STM buffer because the earlier spike pattern representing item A is replaced when afferent spikes appear that represent item D.

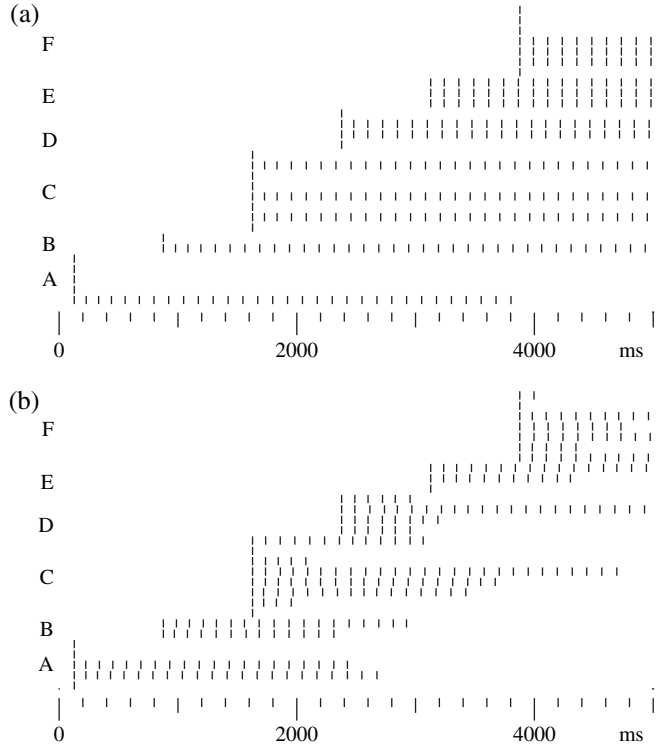


**Figure 17.** Plots of the spike patterns that represent buffered items A–F in the presence of strong noise. (*a*) Strong noise can significantly reduce the number of spikes that represent a buffered item. Between 2 and 8 simultaneous spikes were elicited as items A–F were presented to the buffer by afferent input. Noisy currents affect the membrane potential of pyramidal buffer cells, so that only a subset of each initial spike pattern successfully reactivated due to the ADP response. The buffer capacity was set to 4 items, but noise affected detection of the full buffer state during the theta cycle in which item E was introduced. The buffer therefore maintained reduced representations of items A–E in order until item replacement removed item A. Consequently, the reactivated spike representation of item F merged with the spike pattern for E. (*b*) As the signal to noise ratio was decreased further, the noise also limited the perceived duration of STM. Failed spike reactivation terminated the maintenance of each item representation before the presentation of a fifth item to a full buffer could trigger the item replacement mechanism (which otherwise should have terminated the bottom spike in A first). Despite this, the simulation achieved a noisy FIFO buffering of sequences of 3–4 representations of the items A–F in which order was largely undistorted.

## Discussion

We hypothesize that persistent firing characteristics of pyramidal cells in ECII can provide a reliable short-term buffer for tasks in which encoding of autoassociative and episodic memory depends on the rapid acquisition and maintenance of novel item representations. We propose an explicit mechanism for the FIFO ordered replacement of items in a buffer filled to capacity, and we show that the buffer mechanism can be specified with a range of parameter values and modifications of its specific function.

As in previous simulations by Lisman and Idiart (1995) and by Jensen et al. (1996), our results show (Fig. 6) that the buffer function is achieved without dependence on synaptic modification. Patterns of simultaneous spikes are acquired from a single presentation of input and maintained by persistent firing, regardless of the number of spikes that represent an individual item. The individual items are maintained in their order of presentation, separated from each other by competitive inhibition within a time-compressed sequence of spike patterns. In our previous work (Koene et al. 2003), we clearly demonstrated the benefits of combining nested oscillation at theta and gamma frequencies with repeated spiking that is made possible with ADP currents. Although ADP may sustain repeated reactivation of firing patterns, ADP alone cannot keep successive buffered patterns separated. Competitive inhibition between successive patterns is essential to maintain uncorrupted STM. This is especially true in the realistic case where firing times shift due to noise. Oscillations at gamma frequency are modeled as an emergent characteristic of such competitive inhibition. Theta oscillations are proposed to have a system-level function due to their presence in many regions of the brain (at different phase offsets). Modulating effects at theta rhythm can maintain synchrony between operations in multiple connected networks. This is necessary in particular if rapidly alternating encoding and retrieval is to be achieved (Hasselmo, Bodelon, and Wyble 2002; Hasselmo, Cannon, and Koene 2002; Koene et al. 2003; Koene and Hasselmo 2005). We have now extended these insights into the theoretical model by demonstrating the need for an explicit mechanism that can remove the oldest item in the buffer. Displacement of the oldest item can make room for a new item when novel input appears more rapidly than buffered items are extinguished by other causes, such as noise and slow AHP of the pyramidal cells.

In the simulations by Jensen et al. (1996), new items were presented after the end of the repetition of the items in the buffer, separated by a time interval similar to the duration of one gamma cycle. The input phase in the present model has a similar temporal separation from the last spike during the preceding reactivation of buffer content. Despite this similarity in the input protocol, the addition of new input to a full buffer does not result in the correct FIFO replacement of the oldest item when no additional mechanism is provided for that purpose. A replacement mechanism represented by 2 pyramidal cells and one interneuron is able to perform the FIFO item replacement for buffered item representations with 2–8 spikes. When each node in the model replacement mechanism is expressed as an actual population of neurons, the range of pattern sizes that can be dealt with may be multiplied accordingly.

Three critical parameters of the STM model involve timing that is locked to specific phases of theta rhythm: 1) Input to the buffer must be filtered to appear at a phase that does not interfere with

the reactivation of items in the buffer and that allows the ADP to reactivate new spikes near the end of the same theta cycle. 2) The phase offset of transmission modulation of input to those pyramidal cells that detect a full buffer state determines the working capacity of the buffer. This capacity can be less than the maximum capacity made possible by characteristic theta and gamma frequencies (e.g., compare the 5-item capacity of buffer function in Fig. 5 and the 4-item capacity of buffer function in Fig. 6. The 2 simulations have all parameter values in common [implying the same theoretical maximum capacity] except the size of the phase offset of the transmission modulation of input for the detection of a full buffer, which causes different working capacity). 3) Replacement inhibition must extinguish the reactivation of spikes representing the first item maintained in the buffer, which occurs if the onset of inhibition is at a specific phase of the buffer cycle.

There is some room for biological variability in the parameters of the model that depend on specifics of neurophysiology. The strength of AHP and the timing of the ADP of buffer pyramidal cells may vary within a range of acceptable values. Although transmission modulation is helpful, it is not essential for the rapid alternation of afferent input and reactivation phases in the buffer and may also be replaced in an alternative implementation of the model of the replacement mechanism. The phase sensitivity of neurons that act as the full buffer detector may instead be accomplished by assuring that spiking depends on rhythmic depolarization at theta frequency.

Buffering items in the reverse order of their presentation is a useful modification of the buffer function and was achieved in 2 ways through minor changes of model parameters. Modification of parameters that determine the frequency of theta rhythm and the strength of gamma inhibition directly affects the maximum buffer capacity, and a minimum gamma inhibition is necessary to ensure buffer function that maintains separate items. Beyond this absolute functional minimum strength of competitive inhibition, stronger inhibition and therefore greater intervals of item separation may be desirable for a different reason. Item separation with very small intervals may be problematic when the output of the buffer is used to elicit autoassociative encoding by STDP with a realistic time window for effective synaptic strengthening in a network with recurrent connections. The STDP may lead to unwanted episodic encoding when the time interval between the spike patterns of consecutive items is too small. This reason for a greater minimum strength of gamma inhibition in the model and the consequent realistic nesting of $4 \pm 1$–item reactivation phases per theta cycle are examined in greater detail elsewhere (Koene 2006b, in preparation). The combination of common theta and gamma frequencies lead to buffer capacities in the observed range of $4 \pm 1$ items (Cowan 2001).

Our simulation results predict that the temporal context of items held in STM may be forgotten if an item is presented more than once. This prediction depends critically on 2 presuppositions of the model, namely, 1) the intrinsic nature of item maintenance due to ADP and 2) the explicit replacement mechanism. It may explain specific errors that were observed in rats with prefrontal cortex lesions, but intact entorhinal cortical function, performing a delayed nonmatch to sample task (McGaughy et al. 2005).

Rats without the prefrontal lesions do not exhibit these errors, which may be explained by either of 2 possibilities: 1) The prefrontal cortex may provide an alternative process that can satisfy the task requirements. 2) Prefrontal activity may be involved in a process of multiple instantiation within the parahippocampal and hippocampal systems. For instance, the activity may provide a general or targeted depolarization of neurons in the EC and dentate gyrus, which was implicated in the multiple instantiation of item representations in prior work (Koene 2001) and in a paper that is currently in preparation (Koene 2006c, in preparation). The solution presented there involves the recruitment of spontaneous spikes within the buffer as part of item representations, which may therefore constitute different (though overlapping) sets of spikes for each input presentation. Such a process may solve the general buffering problem encountered when multiple instances of the same input elicit spiking in the buffer with few intervening items (i.e., within buffer capacity).

A theoretical alternative to the ordered reactivation of spike patterns representing successive buffered items is a buffer in which the order of items is represented by the firing rate of spike patterns maintained by persistent firing. A buffer model with such a mechanism is the focus of ongoing study that is based on observed graded persistent cellular activity of pyramidal neurons in ECV (Fransén et al. 2006). A buffer with such a mechanism for the ordered maintenance of items does not appear immediately suitable for the same purposes as our proposed FIFO short-term buffer that is based on cellular activity in ECII and in the neocortex. The output of the present buffer model can drive spiking in recurrent networks in such a manner that episodic associations can be established between successive buffered items. The persistent firing of different items at different frequencies would not obey Hebbian rules that may be expressed by mechanisms of LTP and long-term depression.

We found that buffer performance deteriorates gracefully as the noise that affects the timing of buffer spikes increases. This deterioration takes place in 2 stages: 1) Low levels of noise reduce the number of spikes that represent each item that is maintained in the buffer. 2) High levels of noise also affect the duration of persistent firing in a nondeterministic manner. Consequently, items that are represented by a large number of spikes may be maintained in STM for a longer average period of time than those represented by a small number of spikes. The maintenance of a specific item becomes improbable beyond a duration that is determined by the signal to noise ratio. This feature resembles the assumptions that underlie a theory for the representation of temporal context proposed by Howard and Kahana (2001). A buffer with these characteristics is a useful STM for novel items that must be encoded autoassociatively. When the buffer function is combined with autoassociative retrieval, it is a reliable STM for sequences that are encoded in episodic memory (Koene 2006a, in preparation).

### *Loci of Ordered Short-Term Buffering by Persistent Firing*

ECII is one region in which a short-term buffer mechanism is both needed and plausible: plausible, due to the presence of pyramidal neurons that exhibit ADP and persistent firing and needed, because time compression and repetition of a sequence of spike patterns enable spike-timing–dependent changes to occur at synapses in regions such as ECIII and CA3 that are targets of ECII output. The same buffer mechanism may also be supported in other suitable brain regions such as prefrontal cortex (Andrade 1991). Recent published results confirm the

involvement of the medial temporal lobe cortices in STM for complex relational information (Hannula et al. 2006; Olson, Moore, et al. 2006; Olson, Page, et al. 2006).

The presence of oscillations at theta and gamma frequencies during tasks that involve episodic memory and depend on hippocampal function is supported by electrophysiological evidence (Bragin et al. 1995; Chrobak and Buzsáki 1998; Wyble et al. 2004). ECII provides input to the hippocampal system. There is also evidence that the power of gamma oscillations increases with load in STM (Howard et al. 2003). Persistent firing in response to input stimulation, proposed to occur at theta frequency in pyramidal buffer neurons, has been described in ECII in vitro (Klink and Alonso 1997b) and in EC in vivo (Suzuki et al. 1997; Young et al. 1997). The underlying neurophysiological characteristics of pyramidal neurons in ECII that include an after-depolarizing current were described by Klink and Alonso (1997b) and by Fransén et al. (2002).

From a behavioral perspective, there is a need for extensive episodic encoding. For example, long sequences may be involved in the storage of path memory during a spatial navigation task. Such episodic learning has been shown to depend on hippocampal function (Fortin et al. 2002, 2004). This hippocampal function relies on a short-term buffer for 2 reasons: 1) The interval between the presentation of successive stimuli may vary and may be greater than the maximum time interval for which associations can be made through Hebbian mechanisms at hippocampal synapses. Such an interval may be bridged by short-term buffering. 2) Significant synaptic strengthening occurs only after multiple occurrences of paired pre- and postsynaptic spikes (Wittenberg and Wang 2006) (or postsynaptic dendritic calcium spikes [Kampa et al. 2006]). Prior experiments have shown that the short-term buffer has limited capacity in terms of sequence length (Cowan 2001). Observed behavioral task performance therefore suggests some form of FIFO displacement of buffered items during episodic learning.

### *Scale: A Shift from Dependence on the Number of Spikes to Dependence on the Phase of Spiking*

Scale in terms of the number of neurons in the buffer model has no direct affect on buffer capacity beyond a minimum size requirement. A primary intent of this model is not to be sensitive to the number of spiking neurons but rather to be informed by the phase of spike timing. This was demonstrated through simulations in which item representations within a sequence consisted of different numbers of neurons. Our proposed FIFO mechanism may be replicated within each subregion of local connectivity in a brain region such as ECII. The phase-sensitive parameters of the FIFO mechanism determine buffer capacity. Synchronous operation may be ensured through excitatory connections between components performing the same function of the FIFO mechanism in adjacent subregions: Pf to Pf, Pi to Pi, and Ir to Ir.

Item representations that involve a greater number of neurons can improve the reliability of buffer function. This reliability depends on a minimum separation of items by competitive gamma inhibition during the phase interval of each theta cycle that is the retrieval mode of the buffer. Using experimentally determined values for the theta frequency, this requirement leads to a proposed realistic buffer capacity of $4 \pm 1$ items (Koene 2001, 2006b, in preparation).

The duration of sequence buffering is mainly constrained by the signal to noise ratio, as well as the time constant of the slow after-hyperpolarizing response. In real-world conditions, the duration may more commonly be determined by the rate at which novel input displaces buffered items. This rate can easily exceed the rate at which items would expire due to the slow AHP and noise.

### *Improved Modeling of Realistic Response Mechanisms Affects Functional Requirements*

The neurophysiology modeled here better represents realistic response mechanisms than previous models of persistent spiking buffers that are based on intrinsic mechanisms. Integrate-and-fire neuron dynamics are used in the construction of the present model of STM. These dynamics include a neuronal membrane capacitance that affects the time course of membrane potential when positively or negatively influenced by integrated synaptic responses or intrinsic mechanisms. Capacitance and the leak current were not included explicitly in the buffer models of Lisman and Idiart (1995) and of Jensen et al. (1996) and in work by Koene (2006b, in preparation). This distinction can lead to significantly different requirements that deal with the dynamics of a persistent spiking STM. The capacitance and leak current determine the characteristics of a gradual return of membrane potential to the resting potential. They temporally constrain the cumulative effect of changes in the membrane potential caused by postsynaptic responses and intrinsic mechanisms that are initiated at different times.

The proposed method of item replacement requires that the first item maintained in STM reactivates at the earliest phase at which the combination of depolarizing theta modulation and ADP reaches threshold and that the duration of a theta period is approximately equal to the rise time of the ADP. The first requirement is guaranteed after few cycles of item reactivation because the theta response assures that item reactivation shifts to its earliest possible phase.

The functional requirements of item replacement in the buffer model are also changed by the increased realism of our model. In contrast with the present model, Jensen et al. (1996) assumed one homogeneous population of interneurons that act as a single network-wide inhibitor in response to an action potential of any pyramidal neuron. They postulate that this one mechanism of network inhibition is responsible both for the observed gamma oscillations and the suppression of the oldest item in a STM buffer when novel input causes pyramidal spiking after the last cycle of sequence reactivation. Because the delay of spike propagation and the response timing of a single mechanism are fixed, this means that spiking for novel input must occur no earlier than one gamma interval prior to the onset of the next cycle of sequence reactivation. As we showed, such timing does not allow the novel item to reactivate in the same theta cycle, which leads either to the inability to maintain a representation of the novel item or to reverse-order buffering if the time constant of rising ADP is sufficiently great. Therefore, we present the item replacement mechanism that involves a second subset of the interneurons in ECII. We predict that these interneurons activate irregularly and less frequently, namely, in those specific cases when STM capacity has been reached and novel input must be acquired in STM.

### *Neuroanatomical Support for Phase-Specific Inhibition in EC as Required by the Item Replacement Mechanism*

Many different types of interneurons have been identified in the medial temporal lobes (Freund and Buzsaki 1996; Gulyás et al.

1999). Two of these types of interneurons are believed to be involved in the nested theta and gamma rhythms in the hippocampal system (White et al. 2000). Recent observations have shown that some groups of specific interneuron types (such as CB1-expressing interneurons) predominantly spike irregularly. We predict that such interneurons may be preferentially active at specific phases of the theta cycle and the specific phase can differ as needed. We presuppose this differentiation between populations of interneurons, which play different functional roles in the EC. One population of interneurons may provide the inhibitory feedback that is detected as the gamma rhythm, whereas another population of interneurons may conditionally provide inhibition that suppresses first item activation in a persistent spiking buffer in ECII.

Previous models (Jensen et al. 1996) require that each buffered item is represented by the same number of spiking neurons, an assumption that may not be warranted. In any case, the simulations with noise in this paper clearly show that items would "not be represented by the same number" of simultaneously spiking neurons after arbitrary spikes drop out due to noise, even if the initial numbers were the same. A robust short-term buffer model should be able to maintain and replace items in order that are represented by different numbers of spiking neurons. In the present model, functions such as the detection of a full buffer that can lead to item displacement if novel input appears are not sensitive to threshold numbers of buffered spikes but are instead sensitive to spiking beyond a specific phase of the theta cycle. This constitutes a significant advance compared with previous neural network models of associative memory function, almost all of which assume that the same number of neurons represents each pattern. The assumption that varying numbers of neurons can represent different items is also more consistent with unit physiology. For example, Young et al. (1997) recorded from 378 units, 128 of which were in the EC. Of these, the activity of 91.4% of the EC units could be related to 1 of 4 behavioral events in a delayed nonmatch to sample task with statistical significance. There was no evidence of representation by similar numbers. The number of categorized units for each type of event in the sample was different. For instance, the sample contained 3 units of the "match–nonmatch reward approach" category and 10 units of the "response cue–sampling cells" category.

### *The Repeated Appearance of Spikes Caused by Afferent Input Can Lead to a Reduction of Buffer Content*

Our default parameter values specify a theta cycle duration and strength of gamma inhibition with which the maximum achievable buffer capacity is to sustain the firing of 5 items (detecting full state at a phase offset of 103 ms). When item replacement occurred in a buffer filled to maximum capacity ($N_{max}$), we observed a toggling of the number of items maintained in the buffer, between $N_{max}$ and $N_{max} - 1$. In the case where $N_{max} = 5$, the buffer can accept and maintain a fifth item when it contains only 4 items. If the buffer is already full, then another input causes replacement inhibition that suppresses the first item, but the new item presented by afferent input cannot reactivate in the buffer during that theta cycle because the item reactivation phases for items 2 to $N_{max}$ are still occupied. The buffer maintains the remaining 4 spike patterns until another input arrives, which is then maintained in the fifth reactivation phase. Maintaining $N_{max}$ items can therefore depend on a specific input protocol, which requires 2 presentations of novel input once the buffer is full. Robust capacity with no special input protocol requirements and our proposed default parameter values is therefore $N = 4$ items (achieved by detecting full state at a phase offset of 84 ms). At that capacity, the depolarizing phase of theta modulation in buffer pyramidal cells extends sufficiently beyond the $N$th item reactivation phase to enable a new item representation to reactivate in the same theta cycle.

### *Noisy STM Is Sufficiently Reliable to Support Encoding by STDP*

In the presence of noise, we predict that the maintenance of ordered patterns of spikes in the buffer deteriorates gracefully in the sense that the buffer output provided by cycles of pattern reactivation (Fig. 17*b*) can enable encoding of an episodic representation in a recurrent network through STDP. This graceful deterioration is marked by noise errors that are predominantly categorized as the loss (or dropout) of spikes in representative spike patterns, rather than the splitting of patterns or changes in the order of maintained spikes. The latter type of errors would be more problematic because they could lead to false associations through synaptic modification by STDP. Specific reasons for the predominance of dropout errors are the following: 1) Greater sensitivity of the buffer to the timing of the reactivation of the first item because the combination of depolarization by theta modulation and peak ADP is just sufficient for reactivation at the first item phase. 2) The overall tendency that the earliest spikes within a noisy pattern of near-simultaneous spikes lead to competitive suppression durable enough to prevent spiking of the suppressed neurons, especially during the reactivation phase interval of the first item. 3) Errors in later item spike patterns that are also maintained in the buffer are more able to produce problematic shifts instead of dropout, but are less likely to occur, due to stronger depolarization at later phases of theta modulation and a phase of the spike onset that is constrained by preceding gamma inhibition.

When item separation deteriorates, as shown for the case of insufficient gamma inhibition in Figure 12, the merged spiking output of the buffer no longer induces episodic encoding. Target regions with recurrent synapses modified by spike-timing–dependent plasticity may then erroneously encode a single autoassociative representation for the merged patterns of spikes.

When the recurrent gamma inhibition is sufficiently strong, decoherence of a spike pattern that represents an item may occur more rapidly if there is a significant difference between the amount of recurrent inhibition that is received by different buffer neurons that participate in the pattern of spiking. Order remains sensible even if decoherence leads to the temporal separation of a spike pattern into several parts. Successive parts of a spike pattern that were elicited by a specific item input are all reactived prior to the reactivation of the spike pattern (or sequence of partial patterns) that was elicited by the next input. Furthermore, item buffering is sustained as long as a sufficient number of simultaneous spikes represent the item, despite the common occurrence of spike dropout in the case of decoherence (due to noise or other causes). By definition, simultaneously reactivating spikes are the representation of a specific input. With regard to the issue of the strength of recurrent

inhibition, the similarity of recurrent inhibition received is therefore a precondition for spiking neurons to be considered members of an item representation, a self-selective process.

The simulations presented in this paper use an explicit integrate-and-fire model of a single interneuron to represent the network of interneurons in ECII that is responsible for competitive inhibition, as in previous (Koene 2001) and related (Koene 2006b, in preparation) work and based on the model of Lisman and Idiart (1995). The influence of the competitive gamma inhibition tends to compress shifting spike phases back into synchrony. Beyond certain limits, a shift of spike phase may cause degradation of a spike pattern, as described above. We suggest that an item represented by a sufficiently large population of spiking neurons does not degrade critically over the time span of STM. Additionally, one of the effects of repeated synchronized spikes in an ECII buffer may be to strengthen recurrent excitatory synapses there. Jensen et al. (1996) used such synaptic modification during persistent spiking in a different model of STM. We continue to investigate this possible use of the recurrent excitatory fibers in ECII.

The noisy maintenance of 3–4 items in Figure 17*b*, in a FIFO ordered manner, demonstrates that the buffer provides many theta cycles in which STDP may encode the episodic relationship between consecutive novel items. Deterioration due to noise may be countered in the case when the buffer maintains a sequence of known (previously encoded) autoassociative spike patterns. This is achieved by synaptic modification in sparse recurrent fibers within ECII and by error correction (pattern completion) through the retrieval of stored autoassociative spike patterns in ECIII, to be presented in a separate paper (Koene 2006a, in preparation).

The signal to noise ratio of the system may itself be a significant characteristic of the mechanism. For instance, a STM buffer may not need to develop a phase-locked mechanism for item replacement in the presence of strong noise. Such a replacement mechanism would only be needed if the rate at which item replacement by new input is desired is faster than the rate at which all spikes of the oldest item in the buffer are extinguished by the effects of noise. Unfortunately, strong noise places greater limitations on the maximum duration of item maintenance in STM. This limitation may be countered by using a larger number of spikes to represent each item, but then an explicit replacement mechanism, as proposed in this study, may again be needed.

The described condition of graceful deterioration with noise is presumed to be the realistic condition. Buffer function is sufficiently robust as long as information is maintained during the required time span of STM. We will include the noisy buffer model with increased population size in subsequent simulations of hippocampal and prefrontal activities. This will allow us to further investigate the ordered self-termination of buffered items due to strong noise.

Further enhancement of short-term buffer models will seek to also replicate non-FIFO displacement phenomena, such as primacy and flat or negative recency effects (Brown 1958; Peterson L and Peterson M 1959; Atkinson and Shiffrin 1968; Glanzer 1972; Davelaar and Usher 2002). Ongoing work that extends the buffer model beyond the description in this paper will include an explicit representation of recurrent excitatory fiber in ECII. Recurrent excitatory activity in an ECII buffer may have a stabilizing effect that benefits item maintenance, an effect considered in prior work by Jensen et al. (1996) and by Koene (2001). Whereas model parameters in the simulations presented here were tuned within plausible ranges, we are also constructing simulations of the proposed buffer pyramidal neurons in ECII with greater biophysical detail (Fransén et al. 2002) and with parameters calibrated to patch-clamp experiments designed to test the model. These steps will enable us to further evaluate the ability of pyramidal neurons such as those in ECII to perform the functions presented in this paper.

## Notes

The CATACOMB simulations described here and information about the CATACOMB environment created and maintained by Robert C. Cannon are available on our Computational Neurophysiology web site at http://askja.bu.edu. This work was supported by National Institutes of Health R01 grants DA16454 (CRCNS), MH60013, and MH61492 to MEH and by NSF Science and Learning Center SBE 0354378 and Conte Center Grant MH60450. *Conflict of Interest*: None delcared.

Address correspondence to R.A. Koene, Center for Memory and Brain, Department of Psychology and Program in Neuroscience, Boston University, 64 Cummington Street, Boston, MA 02215, USA. Email: randalk@bu.edu.

## References

Alonso A, Gaztelu J, Bruno W Jr, Garcia-Austt E. 1987. Cross-correlation analysis of septohippocampal neurons during theta-rhythm. Brain Res. 413:135–146.

Andrade R. 1991. The effect of carbachol which affects muscarinic receptors was investigated in prefrontal layer v neurons. Brain Res. 541:81–93.

Atkinson R, Shiffrin R. 1968. Human memory: a proposed system and its control processes. In: Spence K, Spence J, editors. The psychology of learning and motivation. Vol. 2. New York: Academic Press. p. 89–105.

Bi G, Poo M. 1998. Synaptic modifications in cultured hippocampal neurons: dependence on spike timing, synaptic strength, and postsynaptic cell type. J Neurosci. 18(24):10464–10472.

Bliss T, Collingridge G. 1993. A synaptic model of memory: long-term potentiation in the hippocampus. Nature. 361:31–39.

Bliss T, Lømo T. 1973. Long-lasting potentiation of synaptic transmission in the dentate area of the anaesthetized rabbit following stimulation of the perforant path. J Physiol. 232:331–356.

Bragin A, Jando G, Nadasdy Z, Hetke J. 1995. Gamma (40-100 hz) oscillation in the hippocampus of the behaving rat. J Neurosci. 15:47–60.

Brazhnik E, Fox S. 1999. Action potentials and relations to the theta rhythm of septohippocampal neurons in vivo. Exp Brain Res. 127:244–258.

Brown J. 1958. Some tests of the decay theory of immediate memory. Q J Exp Psychol. 10:12–21.

Buzsáki G, Leung L, Vanderwolf C. 1983. Cellular bases of hippocampal EEG in the behaving rat. Brain Res. 287:139–171.

Cannon R, Hasselmo M, Koene R. 2003. From biophysics to behaviour: Catacomb2 and the design of biologically plausable models for spatial navigation. Neuroinformatics. 1(1):3–42.

Chrobak J, Buzsáki G. 1998. Gamma oscillations in the entorhinal cortex of the freely behaving rat. J Neurosci. 18(1):388–398.

Cowan N. 2001. The magical number 4 in short-term memory: a reconsideration of mental storage capacity. Behav Brain Sci. 24(1):84–114.

Crowder R, Morton J. 1969. Precategorical acoustic storage (pas). Percept Psychophys. 5:365–373.

Davelaar E, Usher M. 2002. An activation-based theory of immediate item memory. In: Bullinaria J, Lowe W, editors. Proceedings of the Seventh Neural Computation and Psychology Workshop: Connectionist Models of Cognition and Perception. Brighton (UK). Singapore: World Scientific. p. 118–130.

Egorov A, Hamam B, Fransen E, Hasselmo M, Alonso A. 2002. Graded persistent activity in entorhinal cortex neurons. Nature. 420(6912):173–178.

Fortin N, Agster K, Eichenbaum H. 2002. Critical role of the hippocampus in memory for sequences of events. Nat Neurosci. 5:458–462.

Fortin N, Wright S, Eichenbaum H. 2004. Recollection-like memory retrieval in rats is dependent on the hippocampus. Nature. 431:188–191.
Fox S. 1989. Membrane potential and impedance changes in hippocampal pyramidal cells during theta rhythm. Exp Brain Res. 77:283–294.
Fox S, Wolfson S, Ranck J. 1986. Hippocampal theta rhythm and the firing of neurons in walking and urethane anesthetized rats. Exp Brain Res. 62:495–508.
Fransén E, Alonso A, Hasselmo M. 2002. Simulations of the role of the muscarinic activated calcium-sensitive nonspecific cation current $i_{NCM}$ in entorhinal neuronal activity during delayed matching tasks. J Neurosci. 22(3):1081–1097.
Fransén E, Tahvildari B, Egorov A, Hasselmo M, Alonso A. 2006. Mechanism of graded persistent cellular activity of entorhinal cortex layer V neurons. Neuron. 49:735–746.
Freund T, Buzsaki G. 1996. Interneurons of the hippocampus. Hippocampus. 6:347–470.
Glanzer M. 1972. Storage mechanisms in recall. In: Bower G, editor. The psychology of learning and motivation: advances in research and theory. Vol. 5. New York: Academic Press. p. 129–193.
Gulyás A, Megias M, Emri Z, Freund T. 1999. Total number and ratio of excitatory and inhibitory synapses converging onto single interneurons of different types in the CA1 area of the rat hippocampus. J Neurosci. 19(22):10082–10097.
Haarmann H, Usher M. 2001. Maintenance of semantic information in capacity-limited item short-term memory. Psychon Bull Rev. 8(3):568–578.
Hannula D, Tranel D, Cohen N. 2006. The long and the short of it: relational memory impairments in amnesia, even at short lags. J Neurosci. 26(32):8352–8359.
Hasselmo M. 2005. A model of prefrontal cortical mechanisms for goal directed behavior. J Cogn Neurosci. 17(17):1115–1129.
Hasselmo M, Bodelon C, Wyble B. 2002. A proposed function for hippocampal theta rhythm: separate phases of encoding and retrieval enhance reversal of prior learning. Neural Comput. 14(4):793–817.
Hasselmo M, Cannon R, Koene R. 2002. A simulation of parahippocampal and hippocampal structures guiding spatial navigation of a virtual rat in a virtual environment: a functional framework for theta theory. In: Witter M, Wouterlood F, editors. The parahippocampal region: organization and role of cognitive functions. Oxford: Oxford University Press. p. 139–161.
Hasselmo M, Eichenbaum H. 2005. Hippocampal mechanisms for the context-dependent retrieval of episodes. Neural Netw. 18(9): 1172–1190.
Hebb D. 1949. The organization of behavior. New York: Wiley.
Howard M, Kahana M. 2002. A distributed representation of temporal context. J Math Psychol. 46(3):269–299.
Howard M, Rizzuto D, Caplan J, Madsen J, Lisman J, Aschenbrenner-Scheibe R, Schultze-Bonhage A, Kahana M. 2003. Gamma oscillations correlate with working memory load in humans. Cereb Cortex. 13:1369–1374.
Jensen O, Idiart M, Lisman J. 1996. Physiologically realistic formation of autoassociative memory in networks with theta/gamma oscillations: role of fast NMDA channels. Learn Mem. 3:243–256.
Jensen O, Lisman J. 1996a. Novel lists of 7 ± 2 known items can be reliably stored in an oscillatory short-term memory network: interaction with long-term memory. Learn Mem. 3:257–263.
Jensen O, Lisman J. 1996b. Theta/gamma networks with slow NMDA channels learn sequences and encode episodic memory: role of NMDA channels in recall. Learn Mem. 3:264–278.
Kahana M. 1996. Associative retrieval processes in free recall. Mem Cogn. 24(1):103–109.
Kamondi A, Acsády L, Buzsáki G. 1998. Dendritic spikes are enhanced by cooperative network activity in the intact hippocampus. J Neurosci. 18(10):3919–3928.
Kampa B, Letzkus J, Stuart G. 2006. Requirement of dendritic calcium spikes for induction of spike-timing-dependent synaptic plasticity. J Physiol. 574(1):283–290.
Klink R, Alonso A. 1997a. Morphological characteristics of layer ii projection neurons in the rat medial entorhinal cortex. Hippocampus. 7:571–583.
Klink R, Alonso A. 1997b. Muscarinic modulation of the oscillatory and repetitive firing properties of entorhinal cortex layer ii neurons. J Neurophysiol. 77(4):1813–1828.
Koene R. 2001. Functional requirements determine relevant ingredients to model for on-line acquisition of context dependent memory [PhD thesis]. Montreal (Canada): McGill University, Department of Psychology. p. 1–199.
Koene R, Gorchetchnikov A, Cannon R, Hasselmo M. 2003. Modeling goal-directed spatial navigation in the rat based on physiological data from the hippocampal formation. Neural Netw. 16(5–6):577–584.
Koene R, Hasselmo M. 2005. An integrate and fire model of prefrontal cortex neuronal activity during performance of goal-directed decision making. Cereb Cortex. 15(12):1964–1981.
Levy W, Stewart D. 1983. Temporal contiguity requirements for long-term associative potentiation/depression in the hippocampus. Neuroscience. 8(4):791–797.
Lisman J, Idiart M. 1995. Storage of 7 ± 2 short-term memories in oscillatory subcylces. Science. 267:1512–1515.
Markram H, Lübke J, Frotscher M, Sakmann B. 1997. Regularion of synaptic efficacy by coincidence of postsynaptic aps and epsps. Science. 225:213–215.
McGaughy J, Koene R, Eichenbaum H, Hasselmo M. 2004. Effects of cholinergic deafferentation of prefrontal cortex on working memory: a convergence of behavioral and modeling results. Program No. 551.7. 2004 Abstract Viewer/Itinerary Planner. Washington (DC). Society for Neuroscience.
McGaughy J, Koene R, Eichenbaum H, Hasselmo M. 2005. Cholinergic deafferentation of the entorhinal cortex in rats impairs encoding of novel but not familiar stimuli in a delayed nonmatch-to-sample task. J Neurosci. 25(44):10273–10281.
Olson I, Moore K, Stark M, Chatterjee A. 2006. Visual working memory is impaired when the medial temporal lobe is damaged. J Cogn Neurosci. 18(7):1087–1097.
Olson I, Page K, Moore K, Chatterjee A, Verfaellie M. 2006. Working memory for conjunctions relies on the medial temporal lobe. J Neurosci. 26(17):4596–4601.
Peterson L, Peterson M. 1959. Short-term retention of individual verbal items. J Exp Psychol. 58:193–198.
Phillips J, Shiffrin R, Atkinson R. 1967. Effects of list length on short-term memory. J Verb Learn Verb Behav. 6:303–311.
Skaggs W, McNaughton B, Wilson M, Barnes C. 1996. Theta phase precession in hippocampal neuronal populations and the compression of temporal sequences. Hippocampus. 6:149–172.
Stewart M, Fox S. 1990. Do septal neurons pace the hippocampal theta rhythm? Neuron. 13:163–168.
Suzuki W, Miller E, Desimone R. 1997. Object and place memory in the macaque entorhinal cortex. J Neurophysiol. 78:1062–1081.
Wallenstein G, Hasselmo M. 1997. Bursting and oscillations in a biophysical model of hippocampal region CA3: implications for associative memory and epileptiform activity. In: Bower J, editor. Computational neuroscience: trends in research. New York: Plenum Press. p. 547–552.
White J, Banks M, Pearce R, Kopell N. 2000. Networks of interneurons with fast and slow γ-aminobutyric acid type a ($gaba_a$) kinetics provide substrate for mixed gamma-theta rhythm. Proc Natl Acad Sci USA. 97(14):8128–8133.
Wittenberg G, Wang SH. 2006. Malleability of spike-timing-dependent-plasticity at the CA3-CA1 synapse. J Neurosci. 26(24):6610–6617.
Wyble B, Hyman J, Rossi C, Hasselmo M. 2004. Analysis of theta power in hippocampal EEG during bar pressing and running behavior in rats during distinct behavioral contexts. Hippocampus. 14(5):662–674.
Young B, Otto T, Fox G, Eichenbaum H. 1997. Memory representation within the parahippocampal region. J Neurosci. 17(13): 5183–5195.